Author
Binh Quang Nguyen
Hong Xuan Do
Hung Thanh Pham
Binh Van Doan
Hien Trong Dieu Le
Tu Hoang Le
Quan Trung Nguyen
Coordinator
Marie-Noëlle Woillez

SEPTEMBER 2026
No 405

Assessment of future flood inundation under the impacts of climate change and human activities in Central Vietnam

Research papers

ÉDITIONS AFD
AGENCE FRANÇAISE DE DÉVELOPPEMENT

Agence française de développement

Papiers de recherche

Les *Papiers de Recherche de l'AFD* ont pour but de diffuser rapidement les résultats de travaux en cours. Ils s'adressent principalement aux chercheurs, aux étudiants et au monde académique. Ils couvrent l'ensemble des sujets de travail de l'AFD : analyse économique, théorie économique, analyse des politiques publiques, sciences de l'ingénieur, sociologie, géographie et anthropologie. Une publication dans les *Papiers de Recherche de l'AFD* n'en exclut aucune autre.

Les opinions exprimées dans ce papier sont celles de son (ses) auteur(s) et ne reflètent pas nécessairement celles de l'AFD. Ce document est publié sous l'entière responsabilité de son (ses) auteur(s) ou des institutions partenaires.

Research Papers

AFD Research Papers are intended to rapidly disseminate findings of ongoing work and mainly target researchers, students and the wider academic community. They cover the full range of AFD work, including: economic analysis, economic theory, policy analysis, engineering sciences, sociology, geography and anthropology. *AFD Research Papers* and other publications are not mutually exclusive.

The opinions expressed in this paper are those of the author(s) and do not necessarily reflect the position of AFD. It is therefore published under the sole responsibility of its author(s) or its partner institutions.

Assessment of future flood inundation under the impacts of climate change and human activities in Central Vietnam

Authors

Binh Quang Nguyen
The University of Danang – University of Science and Technology

Hong Xuan Do
Nong Lam University – Ho Chi Minh City

Hung Thanh Pham
The University of Danang – University of Science and Technology

Binh Van Doan
Vietnamese-German University

Hien Trong Dieu Le
University of Thu Dau Mot

Tu Hoang Le
Nong Lam University – Ho Chi Minh City

Quan Trung Nguyen
The University of Danang – University of Science and Technology

Coordinator

Marie-Noëlle Woillez (AFD)

Abstract
This study evaluates the combined impacts of climate change and reservoir operations on flood dynamics in the Vu Gia Thu Bon River Basin, one of Vietnam's most flood-prone regions. The analysis employs an integrated modeling chain, coupling the SWAT hydrological model with the HEC-RAS 2D hydrodynamic model to simulate streamflow and flood inundation across various scenarios. The SWAT model is forced by statistically downscaled climate projections from 19 CMIP6 GCMs under SSP2-4.5, SSP3-7.0, and SSP5-8.5 scenarios. The analysis focuses specifically on the evolution of flood events associated with a 20-year return period at different Global Warming Levels (GWLs). Climate projections show a significant increase in extreme rainfall by the end of the century, albeit with a large inter-model spread. Hydrological simulations indicate that the current cascade of reservoirs provides a substantial buffering capacity for flood events with a 20-year return period, still reducing peak discharge and flood extent even under 3°C GWL compared to the historical pre-dam period. However, at higher GWL, intensified hydrological extremes and increased downstream rainfall may eventually overwhelm current water management infrastructures. The results underscore the necessity of moving beyond "stationary" flood design assumptions, as the probability of extreme rainfall continues to rise. Ultimately, this research provides a scientific foundation for enhancing social resilience and developing robust flood mitigation strategies in the face of an uncertain climatic future in Central Vietnam.

Keywords
Climate change, Flood inundation, SWAT, HEC-RAS, Vu Gia Thu Bon River Basin, Vietnam, Adaptive water management

Acknowledgements
This study is supported by the 2nd phase of the GEMMES Viet Nam project, funded by the French Development Agency through Facility 2050.

Original version
English

Accepted
September 2026

Résumé
Cette étude évalue les impacts combinés du changement climatique et de la gestion des réservoirs sur la dynamique des crues dans le bassin versant de la rivière Vu Gia Thu Bon, l'une des régions du Vietnam les plus exposées aux innondations. L'analyse repose sur le couplage du modèle hydrologique SWAT au modèle hydrodynamique HEC-RAS 2D afin de simuler les débits et l'inondation pour différents scénarios. Le modèle SWAT est forcé par les projections climatiques de 19 modèles climatiques globaux CMIP6, raffinées par descente d'échelle statistique, pour les scénarios SSP2-4.5, SSP3-7.0 et SSP5-8.5. L'analyse se concentre spécifiquement sur l'évolution des épisodes de crue avec une période de retour de 20 ans, à différents niveaux de réchauffement planétaire. Les projections climatiques indiquent une augmentation significative des précipitations extrêmes d'ici la fin du siècle, avec toutefois une forte dispersion inter-modèles. Les simulations hydrologiques montrent que la cascade actuelle de réservoirs conserve une capacité importante d'atténuation des innondations de période de retour 20 ans, réduisant encore les débits maximums et l'étendue des inondations pour 3°C de réchauffement planétaire par rapport à la période historique antérieure aux barrages. Toutefois, à des niveaux de réchauffement plus élevés, l'intensification des extrêmes hydrologiques et l'augmentation des précipitations en aval pourraient finir par dépasser les capacités des infrastructures actuelles de gestion de l'eau. Les résultats soulignent la nécessité de dépasser les hypothèses « stationnaires » dans la conception des protections contre les innondations face à l'augmentation de la probabilité d'occurrence des pluies intenses. Cette étude fournit une base scientifique pour renforcer la résilience des sociétés et développer des stratégies robustes d'atténuation des inondations face à un avenir climatique incertain dans le centre du Vietnam.

Mots-clés
Changement climatique ; innondations ; SWAT ; HEC-RAS ; Vu Gia Thu Bon ; Vietnam ; gestion adaptative de l'eau.

Remerciements
Cette étude a été soutenue par la deuxième phase du projet GEMMES Vietnam, financé par l'Agence française de développement (AFD) via la Facilité 2050.

Version originale
Anglais

Acceptée
Septembre 2026

Introduction

Floods are one of the most destructive disasters, causing severe environmental degradation and human suffering worldwide. Extreme flood events often cause extensive and sometimes irreversible damage (Pham et al., 2021). Over the past several decades, both economic and environmental losses associated with flooding have risen markedly (Merz et al., 2021). This escalation can be attributed primarily to two factors: the increasing frequency and intensity of rainfall under a warming climate, and the growing population and asset exposure to flood-prone areas driven by socio-economic development (Tabari, 2020). Concerns over hydro-climatic extremes and their impacts have intensified, as climate change is expected to further amplify flood hazards worldwide (Wang et al., 2022). Scientific evidence confirms that with every 1°C increase in air temperature, the atmosphere can hold roughly 7% more water vapor, thereby intensifying precipitation extremes (Seneviratne et al., 2021). Nonetheless, other atmospheric processes such as local moisture availability, regional wind circulation, and the dynamics of tropical weather systems also influence rainfall intensity. Projections of future flood changes are strongly region-dependent, with some parts of the world expected to experience stable or even decreasing flood hazards, whereas Southeast Asia is consistently identified as a region where flood hazards are projected to intensify (IPCC, 2023). Successive assessment reports of the Intergovernmental Panel on Climate Change (IPCC), most recently the Sixth Assessment Report (AR6), highlight with increasing confidence that heavy precipitation events are projected to intensify in the future across global, continental, and regional scales (Seneviratne et al., 2021). Moreover, the AR6 chapter on the water cycle changes (Douville et al., 2021) emphasizes that large flood events are likely to become more severe, even though the relationship between precipitation and flooding remains complex due to catchment characteristics and land use factors. Against this backdrop, research on changing flood risks is crucial, as it provides scientific evidence to support adaptation strategies and enhance social resilience to the evolving impacts of climate change.

In Vietnam, floods are among the most devastating natural hazards, generating extensive environmental and socioeconomic losses (Nguyen et al., 2021). Multiple mechanisms, including prolonged and intense rainfall during the monsoon season, tropical storms and typhoons, and coastal tidal surges, trigger them. One of the most catastrophic historic events was the flood of November 1999 in Central Vietnam, particularly in Thua Thien Hue and Quang Nam provinces, which caused more than 595 fatalities and economic damages estimated at nearly 290 million USD, equivalent to around 1% of the national GDP at the time (ADRC, 2000). A more recent and severe example is the 2020 Central Vietnam floods, which struck between October and November. This disaster was driven by a succession of five tropical cyclones combined with seasonal monsoon rains. It resulted in approximately US$1.4 billion in damages, with 291 deaths and 66 people missing as of mid-November 2020. The floods affected several central provinces, destroyed or damaged hundreds of thousands of homes, overwhelmed infrastructure, inundated croplands, and caused large-scale livestock and poultry losses (IFRC, 2022).

In recent decades, Vietnam has frequently experienced extreme precipitation events, resulting in recurrent flash floods and urban inundation, particularly in the central and northern regions (Luo et al., 2018; Nguyen et al., 2021). Flood risk arises from the combination of flood hazard, exposure, and vulnerability. In the Vu Gia Thu Bon (VGTB) River basin in Central Vietnam, these elements are particularly acute: heavy seasonal rainfall and typhoons (hazard), growing population and infrastructure along low-relief lands (exposure), and limited adaptive capacity, especially in rural and peri-urban communities (vulnerability) (Nguyen et al., 2024). To address this, both scientific studies and government programs have directly targeted mapping hazards, forecasting floods, and integrating flood risk management. For example, Nguyen H.D. et al. (2024) applied machine learning combined with hydrodynamic modelling (using MIKE FLOOD) to assess flood hazard in the VGTB basin for the 2017 flood event. They produced maps of flood depth, velocity, and susceptibility, classifying areas into hazard categories ranging from very low to very high. In the related line of research, Vo and Gourbesville (2016) also used the MIKE-DHI modelling system to simulate the 1999 flood event and produce inundation maps across the basin. Another study evaluated how upstream reservoir operations and ongoing urbanization alter flood inundation: increasing reservoir flood storage reduces flooded area and peak water levels; meanwhile, expansion of urban and road infrastructure aggravates flooding by reducing drainage and increasing flood depth around roads (To et al., 2022). On the policy side, flood hazard maps in the VGTB basin have also been developed under integrated frameworks using the Driver-Pressure-State-Impact-Response (DPSIR) model to show inundation zones for different flood return periods (10-year, 20-year and 100-year return period, associated with 10%, 5%, 1% Annual Exceedance Probability (AEP)) and guide disaster management planning (Pham et al., 2015). Thus, in the VGTB basin, flood risk assessment is being advanced through empirical mapping of hazard, modelling of changes driven by climate and human activities (land use changes and reservoir operation), early warning and decision support systems, and government-led integrated flood management planning.

Methods for calculating flood hazards vary depending on the type and quality of available datasets. Nevertheless, most approaches share a common conceptual framework that generally involves three main steps. First, flood quantiles corresponding to different probabilities of streamflow (e.g., AEP = 1% for a 100-year return period) are estimated, either from observed discharge records at gauging stations or, where such data are lacking, from simulated streamflow generated by hydrological models. Second, hydrodynamic models are applied to simulate flood wave propagation and convert these flood quantiles into maximum water levels in the downstream area. Third, the simulated water levels are overlaid with a digital elevation model (DEM) to delineate inundated areas for specific return periods and ultimately producing flood hazard maps (Mudashiru et al., 2021).

Numerous scientific studies have projected changes in flood risk across spatial scales, ranging from global to continental, regional, and local catchments (Kundzewicz et al., 2019). At the regional level, many assessments have applied climate model outputs as inputs to hydrological models to estimate future flood hazards (Diop et al., 2025; Lima et al., 2023). However, hydrological models alone typically provide only discharge estimates or flow statistics, without direct information on flood characteristics such as inundation extent and flood depth. These parameters require coupling hydrological outputs with hydrodynamic models (Callaghan and Hughes, 2022; Dysarz et al., 2025; Savino et al., 2023; Sharma et al., 2021). The objective of this study is to evaluate the impacts of climate change and reservoir operations on the flood extent and flood depth in the VGTB River basin, Central Vietnam. To achieve this, we coupled a hydrological model (SWAT) with a hydrodynamic model (HEC-RAS), forming an integrated modelling chain that enables simulation of flood dynamics under future climate conditions. Statistically downscaled and bias-corrected climate change scenarios up to 2099 were propagated through this framework to estimate changes in flood extent and flood depth. The coupling of hydrological and hydrodynamic modelling for climate change impact assessment in this basin provides more robust insights into future flood hazard patterns. In this paper, we present detailed flood hazard maps for the VGTB River basin, depicting inundation extents and depth classes for a historical reference period (1995–2014) as well as for three future climate scenarios (SSP2-4.5, SSP3-7.0, and SSP5-8.5) over the horizon 2015–2099 with the flood quantile of 5% AEP corresponding to a 20-year return period. We also provide analysis of future changes at three Global Warming Levels (GWL), i.e., +2°C, +3°C, and +4°C above preindustrial. These projections provide critical spatial information for evaluating how climate change may alter flood dynamics in one of Central Vietnam's most vulnerable river basins.

The added value of this study lies in three choices. First, rather than reconstructing individual historical or design floods, as previous assessments in the basin have done, we propagate a 19-member CMIP6 ensemble under three emission scenarios through a coupled hydrological–hydrodynamic chain, so that climate-model uncertainty is carried all the way to inundation extent and depth. Second, results are organised by global warming level rather than by time slice, which makes them largely independent of the emission pathway and allows the exercise to be read as a stress test of the current flood-management system. Third, by contrasting the current reservoir cascade with a simulated pre-dam reference, the design separates the climate signal from the effect of infrastructure, and quantifies the share of downstream flooding that reservoir operation cannot control.

1. Study Area and Data

1.1. Study Area

1.1.1. Geography

The Vu Gia Thu Bon (VGTB) River basin, one of the nine largest basins in Vietnam, covers an area of approximately 10,350 km² across Quang Nam province and Da Nang city, and a small part of Kon Tum province in Central Vietnam (Nguyen et al., 2023b, 2024a). The regional topography can be classified into four principal types: high mountainous terrain, high hilly terrain, low hilly terrain, and plains, which are structured around the Vu Gia and Thu Bon river basins. High mountainous terrain is predominantly distributed in the northwestern and southwestern parts of the basin and comprises a series of mountain ranges aligned in a northwest–southeast orientation. These ranges belong to the Truong Son mountain system and exhibit average elevations between 500 and 1,000 m, with several prominent peaks, including Ngoc Linh, the highest at 2,567 m. The high mountain zone generally slopes from west to east and from north to south, with elevations progressively decreasing toward the southeast (Figure 1.a). The basin originates in the Ngoc Linh Mountain, and its river system flows eastward through moderately flat coastal plains.

The Vu Gia and Thu Bon rivers converge about 36 km upstream of the coast, discharging primarily through the Cua Dai Estuary near Hoi An city, while a network of distributary channels connects their lower reaches to the Han Estuary in Da Nang city (Vu et al., 2017). Urban centres such as Hoi An City and Da Nang City are predominantly situated along downstream river channels on low-lying terrain, a configuration that poses substantial constraints on flood drainage capacity in downstream areas. The low-relief topography results in reduced flow velocities, promoting sediment accumulation in estuarine zones, which further diminishes drainage efficiency. Moreover, these urban areas are characterized by high population densities, and associated anthropogenic activities encroach upon and constrict natural flood conveyance channels, thereby exacerbating the reduction in flood drainage capacity. Land use within the basin is dominated by forest, accounting for approximately 74 % in Da Nang and 88 % in Quang Nam, followed by cropland (9 % and 8 %, respectively) and built-up areas (11 % and 2 %) (Figure 2). During the flood season, the Vu Gia and Thu Bon rivers interact via the Quang Hue and Vinh Dien channels, forming a braided deltaic system in the lower basin (Nguyen et al., 2025a, 2024b). Over the past two decades, numerous water supply, hydropower, and other large-scale hydraulic infrastructures have been constructed within the VGTB River basin (Figure 1.b). The development and operation of these structures have substantially altered the basin's hydrological regime under changing climatic conditions, particularly by modifying flow patterns during both low-flow seasons and flood periods (Nguyen et al., 2023a). A summary of the databases providing dam and reservoir information is provided in Table A1 in the Appendix.

1.1.2. Climate and flood regime

The VGTB River basin experiences a tropical monsoon climate characterized by distinct wet and dry seasons (Fig.A.3), which exert a dominant influence on its hydrological regime (Nguyen et al., 2025b, 2025c, 2025d). Annual precipitation varies geographically, with higher rainfall in the upstream mountainous areas and progressively lower values toward the coastal plains (Phuong et al., 2020). Surface water availability in the basin is directly linked to seasonal precipitation patterns, reflecting a strong precipitation–runoff relationship. Approximately 70 % of the annual discharge occurs during the wet season (September–December), when intense monsoonal rainfall drives high runoff (see Appendix 1). In contrast, only about 12 % of the annual runoff occurs during the peak dry season (February–March), due to markedly reduced rainfall and diminished baseflow contributions (Ilyas et al., 2021; Vu et al., 2017).

The flood regime of the Vu Gia Thu Bon River system is characterized by rapid, high-magnitude floods concentrated between September and December, driven by intense rainfall and frequently causing deep inundation in downstream and coastal areas. The basin exhibits high annual runoff (more than 2,000 mm) and strong downstream tidal influence. The flood season is short but accounts for approximately 60–70% of the annual runoff and is characterized by frequent, closely spaced events that produce multi-peaked hydrographs. On average, four or more floods of level I[1] or higher occur annually, with extreme years experiencing up to eight to nine events, resulting in recurrent and compound flooding. Hydropower development, sand mining, and climate change have further increased hydrological complexity, while the combined effects of extreme rainfall, tropical storms, high tides, and steep topography produce a highly hazardous flood regime (Nguyen, 2023b) (see Appendix 2 for more details on recent flood events).

[1] Flood alert levels in Vietnam are station-specific water-level thresholds defined by Decision No. 05/2020/QD-TTg of the Prime Minister, which classifies flood severity into three levels (I, II and III) and triggers progressively stronger disaster-response obligations for local authorities. Level I is the lowest, marking the onset of flooding of low-lying riparian land; level III denotes a dangerous flood affecting settlements and infrastructure, and events exceeding it are reported as "above alert level III". For the stations used in this study, alert level I corresponds to a water level of 14.5m at Hoi Khach and 6.5 m at Ai Nghia on the Vu Gia River; and of 11.0 m at Nong Son, 6.5 m at Giao Thuy, 2.0 m at Cau Lau and 1.0 m at Hoi An on the Thu Bon River.

Figure 1. (a) Topography and river network of the VGTB River basin and (b) schematic map of the river network with hydropower plants and key hydrometeorological stations.

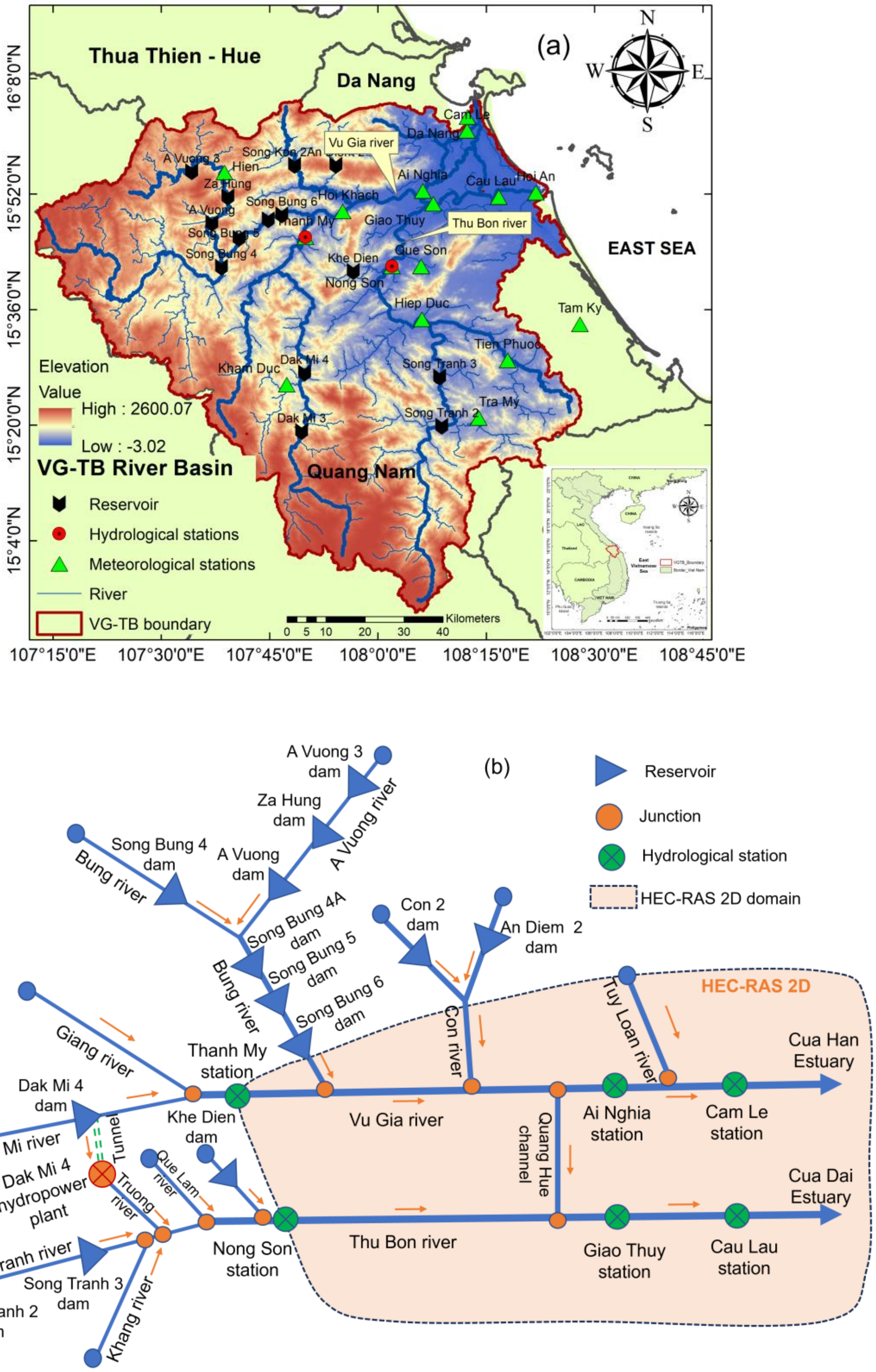

Source: (a) adapted from Nguyen et al. (2024b)

1.2. Input Datasets

1.2.1. Topographical data

Topographic information represents a fundamental input for both hydrological and hydraulic modelling, as it governs the spatial distribution of surface runoff within a catchment and controls flood extent, depth, and flow dynamics during inundation events. Such information is commonly derived from Digital Elevation Models (DEMs), which provide a quantitative representation of terrain morphology. DEMs can be generated through various methods, including ground-based surveying, digitalisation of existing topographic or contour maps, photogrammetric techniques, and remote sensing. In recent years, remote-sensing technologies have become the predominant source of DEM data due to their broad spatial coverage, improved accuracy, and cost-effectiveness (Pham et al., 2018).

Table 1. Summary of topographical data, soil information, and land use data

No	Data type	Sources
1	DEM (30x30 m) of the hydrological model domain, digitalised from 1: 10,000 spot heights	Ministry of Natural Resources and Environment obtained in 2016
2	DEM (5x5m) of the hydraulic model domain derived from high-resolution LiDAR	Reuse DEM from "Building a flood map downstream of reservoirs in the Vu Gia - Thu Bon River basin project" obtained in 2018
3	River cross-section (186 cross sections) used for the hydrodynamic model	https:// www.apn-gcr.org/project/integrated-flood-and-sediment-management-in-river-basins-for-sustainable-development/
4	Soil map (30x30m) (obtained in 2016)	Vie 08-P1 project: Building a GIS database on climate change research results
5	Land use map of the entire province of Quang Nam (16 districts), Da Nang (5 districts), and Kon Tum (1 district) (10x10m) (obtained in 2020)	JAXA (https:// www.eorc.jaxa.jp/ ALOS/en/dataset/lulc_e.htm)

This study used spot height datasets with a scale of 1:10,000 (MoNRE, 2016) to digitalise a DEM (30 m x 30 m) for the hydrologic model. A high-resolution DEM (5 m x 5 m) derived from LiDAR data (APN, 2021) and 186 river cross-sections (Figure A.5) along the analysed reach over the downstream river basin were used to generate bathymetry (including main channel and floodplains) for the hydraulic model. These DEMs were extracted to obtain various topographical (e.g., elevation, slope, or aspect) and hydrological parameters (e.g., flow direction, catchment area, and flow length) as required inputs in hydrological and hydraulic models (Nguyen et al., 2024b, 2025c).

1.2.2. Soil and land use data

Soil information used in this study was obtained from the LUCCi project[2] dataset, which provides a detailed soil classification for the VGTB River basin at a spatial resolution of 30 m. The dataset categorises soils into six major types, reflecting the basin's diverse geomorphological and climatic conditions. Most of the basin is dominated by silt loam and clayey soils, which are characterised by relatively low infiltration capacities and consequently high surface runoff potential (Nguyen et al., 2023a, 2025d).

Figure 2. Land use and land cover map of Quang Nam-Da Nang city for 2020.

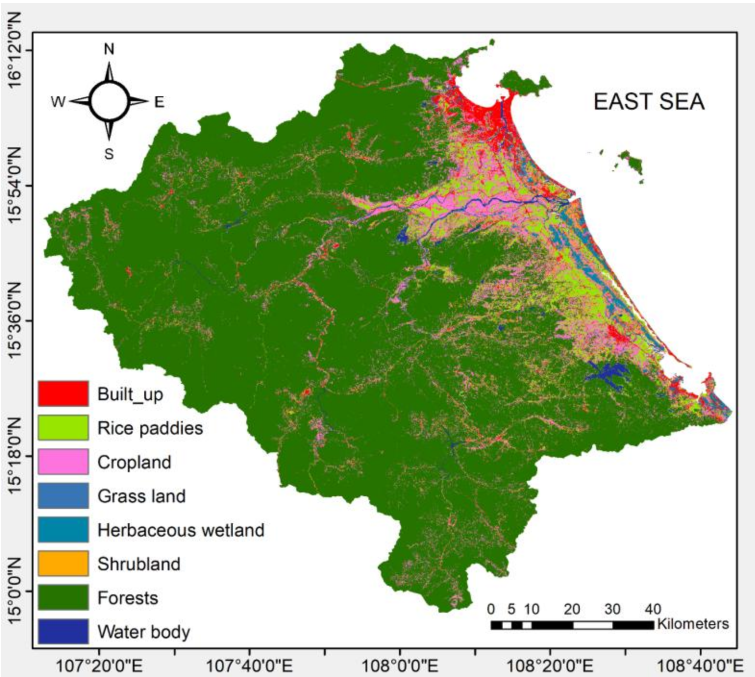

Source: JAXA high resolution land use and land cover map.

Land use and land cover (LULC) data were obtained from the Japan Aerospace Exploration Agency (JAXA) High-Resolution Land Use and Land Cover Map for 2020[3], with a spatial resolution of 10 m. This dataset was used to parameterize surface characteristics in both the hydrological and hydraulic models, including the runoff coefficient, Manning's roughness

[2] http:// www.lucci-vietnam.info/

[3] https:// www.eorc.jaxa.jp/ALOS/en/dataset/lulc_e.htm

coefficient, and runoff curve number (CN). The upstream areas of the VGTB River basin are primarily forested, while cropland dominates the downstream floodplain (Figure 2). Forest cover typically reduces surface runoff through interception, infiltration, and evapotranspiration processes, whereas croplands tend to increase runoff potential due to lower canopy density and reduced infiltration capacity.

1.2.3. Meteorological data

Meteorological inputs, including rainfall, air temperature, humidity, and evapotranspiration, were obtained from the Central Regional Hydro-Meteorological Center[4] from 1976 to 2023. Daily rainfall data from 16 stations (Cam Le, Da Nang, Hien, Thanh My, Hoi Khach, Giao Thuy, Ai Nghia, Cau Lau, Hoi An, Nong Son, Que Son, Hiep Duc, Kham Duc, Tien Phuoc, Tra My and Tam Ky) distributed across the basin, while other daily meteorological data such as air temperature, humidity and evapotranspiration from 3 stations (Da Nang, Hoi An and Tam Ky) were used to drive the hydrological model. These data were quality-checked for continuity and consistency before being used as input data for the hydrological and hydrodynamic models (Nguyen et al., 2023a, 2025a). Because the Soil and Water Assessment Tool (SWAT) model uses hydrologic response units (HRUs, land area sharing similar surface slope, land use, and soil type attributes) as the foundational units for hydrological processes modelling, we assigned climate data input for each subbasin using the closest station to the subbasin centroid. The elevation method is used to take into account the spatial variability of rainfall and temperature within the subbasin, where different elevation zones within the subbasin might experience different rainfall and temperature levels, and then weight the rainfall based on the area of each zone. Each subbasin has a maximum of one weather station, thus all HRUs within the subbasin have the same climate input data. In general, this might lead to inaccurate representation of subbasin rainfall input data, particularly in river basins with complex topography. This method will accurately represent the spatial variability of rainfall if the subbasin delineation sufficiently incorporates the density of observed rainfall stations. In this study, a network of 16 rain gauge stations, relatively evenly distributed across the VGTB basin, ensures that the spatial variability of rainfall is sufficiently captured.

[4] https:// kttvtrungbo.org.vn

Table 2. Summary of meteorological and hydrological data.

No	Data type	Availability period/ Time step	Sources
1	Rain gauge data	1979–2023/ Daily	The Mid-Central Regional Hydro-Meteorological Center, Vietnam
2	Observed temperature, humidity, and evaporation data	1979–2023/ Daily	
3	Observed streamflow data	1979–2023/ Daily	
4	Observed water level data	1979–2023/ Daily 2020/ Hourly	
5	Observed tide level data	1979–2023/ Hourly	
6	Flood trace survey data	2009, 2013, and 2020	
7	Hydraulic structures (dams, levees, bridges, culverts, weirs)		Department of Construction and the Department of Planning and Investment in Da Nang

1.2.4. Hydrological data

Observed streamflow data were collected from 2 stations (Thanh My and Nong Son), managed by the Central Regional Hydro-Meteorological Center, within the VGTB river basin. The records span 48 years (1976-2023), providing continuous daily discharge observations used for calibration and validation of the hydrological model. Peak discharge data for the 2020 historical flood event was also incorporated to evaluate the performance of the coupled hydrological–hydraulic framework in reproducing flood magnitude and extent.

Hourly river stage data from 1976 to 2023 were obtained from seven gauging stations (Thanh My, Nong Son, Giao Thuy, Cau Lai, Hoi Khach, Cam Le, and Hoi An), while tide level data were collected from the Son Tra and Cua Dai stations. All monitoring stations are operated by the Central Regional Hydro-Meteorological Center (Nguyen et al., 2023a, 2025d).

1.2.5. Hydraulic structures data

In the hydraulic model, key infrastructure elements—including dams, levees, bridges, and weirs—were explicitly represented to capture their influence on flow dynamics and flood propagation. These structures modify natural flow patterns by diverting, attenuating, or impounding water, thereby affecting downstream flooding and water resource management. Accurate representation of such features is essential for reliable simulation of flood extent and depth. Detailed geometric and hydraulic information on the major hydraulic structures within the VGTB River basin was obtained from the Department of Construction and the Department of Planning and Investment in Da Nang, Vietnam. There are 18 reservoirs which were constructed and became operational between 2008 and 2020 in the VGTB River basin (Nguyen et al., 2023a) (Table A.2). These data were incorporated into the computational grid of the hydraulic model to ensure an accurate representation of structural effects on flow dynamics (Nguyen et al., 2023b, 2024a-c).

1.2.6. Observed flood trace data

Flood trace observations are essential for post-event analysis, supporting flood mapping, damage assessment, and model validation. In this study, flood trace data from the 2020 flood event were obtained from the Mid-Central Regional Flood Management and Operation Center, Vietnam, and used to validate the simulated flood extent produced by the hydraulic model. The locations of flood trace data collection for the 2020 flood event are shown in the Appendix (Figure A.4).

1.3. Climate Change Scenarios

1.3.1. Temperature and rainfall projections

An investigation of the potential changes in runoff over the VGTB River basin requires projections of future changes in precipitation and temperature. We used the daily temperature and precipitation projections from 19 bias-corrected and statistically downscaled (10 km) CMIP6[5] General Climate Models (GCMs) available through the CMIP6-VN database (Tran-Anh et al., 2023) (Table 3).

We selected GCMs with output data available for both the historical (1980–2014) and future (2015–2099) time-periods under three Shared Socioeconomic Pathways (SSP) (Riahi et al., 2017):

- SSP2-4.5, a medium emission scenario with partial mitigation efforts leading to a best estimate of a 2.7°C global temperature rise above the preindustrial level by the end of the century (2081–2100) (IPCC, 2023);
- SSP3-7.0, a high emission scenario with limited climate policies where global temperature would rise by ~3.6°C by the end of the century;
- SSP5-8.5, a very high emission scenario based on fossil fuel development, which would lead to a warming of ~4.4°C by the end of the century.

[5] Coupled Model Intercomparison Project Phase 6.

We note that, in the ongoing CMIP7 exercise, SSP5-8.5 has been assessed as an implausible emissions pathway (van Vuuren et al., 2026). Its use here is nevertheless justified because our analysis is based on global warming levels rather than scenario likelihood. We use SSP5-8.5 to sample the upper end of the warming range for stress-testing, as 4°C is reached by only a limited number of model–scenario combinations, mostly under SSP5-8.5 (see Table 3). Furthermore, higher climate sensitivity than the current IPCC best estimate cannot be ruled out (Gyuleva et al., 2026), meaning that warming levels associated with SSP5-8.5 remain plausible even if its emissions trajectory is not. Lower-emissions pathways could likewise result in very high warming under higher climate sensitivity. Thus, warming levels above 3°C remain relevant for risk assessment and long-term planning and adaptation.

Future climate forcing from the CMIP6-VN dataset was incorporated into the hydrological SWAT model by spatially linking gridded climate projections to the hydrological model domain. Daily gridded climate forcing inputs for each subbasin were computed using a spatial area-weighted averaging method that explicitly accounts for the fractional area of each grid cell intersecting the subbasin boundary in the SWAT model. The extracted climate series were then assigned uniformly to all hydrological response units (HRUs) within each subbasin.

The CMIP6 climate models offer a new and improved representation of processes and a higher spatial resolution relative to the previous generation (CMIP5). However, a subset of models shows a climate sensitivity above the "likely" or even the "very likely" range assessed in IPCC AR6 based on multiple lines of evidence. Hence, using the ensemble mean of CMIP6 models for regional climate impact assessments may lead to an overestimation of the magnitude of change. To overcome this issue, in this study, we follow the new IPCC (2021) approach and the recommendations of Hausfather et al. (2022), and we complement scenario-based analyses with projections based on global warming levels (GWLs) rather than on scenario and time period.

GWLs are defined by comparing the global mean surface air temperature – computed over a 20-year future period to minimize short-term variability – with that for the preindustrial period 1850–1900. In this study, we focus on GWL 2°C, 3°C, and 4°C above the preindustrial level. The beginning and end years are estimated for each GCM and SSP scenario (see Table 3). Note that the timing of a given GWL depends on both the GCM considered and the SSP scenario. The climate response pattern for a specific GWL is then analysed across all models and scenarios that reach that GWL.

Table 3. Climate models and SSP scenarios used in this study and the 20-year periods corresponding to specific global warming levels.

GCM	GWL 2deg			GWL 3deg			GWL 4deg		
	SSP2-4.5	SSP3-7.0	SSP5-8.5	SSP2-4.5	SSP3-7.0	SSP5-8.5	SSP2-4.5	SSP3-7.0	SSP5-8.5
ACCESS-ESM1-5	2036-2055	2039-2058	2030-2049	NA	2060-2079	2051-2070	NA	NA	2069-2088
AWI-CM-1-1-MR	2030-2049	2028-2047	2027-2046	NA	2055-2074	2050-2069	NA	NA	2070-2089
BCC-CSM2-MR	2048-2067	2037-2056	2034-2053	NA	2065-2084	2056-2075	NA	NA	NA
CanESM5	NA	NA	NA	2040-2059	2034-2053	2031-2050	2074-2093	2050-2069	2045-2064
CMCC-ESM2	2029-2048	2030-2049	2024-2043	2057-2076	2054-2073	2043-2062	NA	2078-2097	2060-2079
CNRM-CM6-1-HR	2024-2043	2023-2042	2020-2039	2053-2072	2048-2067	2042-2061	NA	2067-2086	2057-2076
CNRM-ESM2-1	2046-2065	2043-2062	2036-2055	2079-2098	2063-2082	2055-2074	NA	2080-2099	2070-2089
EC-Earth3	2035-2054	2029-2048	2026-2045	2076-2095	2054-2073	2048-2067	NA	2075-2094	2064-2083
EC-Earth3-Veg	2024-2043	2023-2042	NA	2058-2077	2048-2067	2041-2060	NA	2067-2086	2058-2077
FGOALS-g3	2056-2075	2037-2056	2038-2057	NA	2075-2094	2065-2084	NA	NA	NA
GFDL-ESM4	2064-2083	2048-2067	2043-2062	NA	2074-2093	2066-2085	NA	NA	NA
GISS-E2-1-G	2022-2041	2024-2043	2020-2039	2072-2091	2057-2076	2047-2066	NA	NA	2069-2088
INM-CM5-0	2063-2082	2041-2060	2037-2056	NA	2075-2094	2065-2084	NA	NA	NA
IPSL-CM6A-LR	2024-2043	2025-2044	2025-2044	2056-2075	2046-2065	2041-2060	NA	2067-2086	2057-2076
MIROC6	2064-2083	2050-2069	2044-2063	NA	NA	2067-2086	NA	NA	NA
MIROC-ES2L	2054-2073	2046-2065	2038-2057	NA	2075-2094	2061-2080	NA	NA	NA
MPI-ESM1-2-HR	2054-2073	2041-2060	2040-2059	NA	2072-2091	2064-2083	NA	NA	NA
MRI-ESM2-0	2040-2059	2036-2055	2029-2048	NA	2064-2083	2055-2074	NA	NA	2074-2093
UKESM1-0-LL	2025-2044	2022-2041	2022-2041	2050-2069	2041-2060	2037-2056	NA	2060-2079	2051-2070

Note: NA values indicate that the model does not reach the GWL within the assessment period (from 2020 to 2099)

1.3.2. Sea level rise projections

For sea-level rise (SLR) projections, this study used data from Vietnam's official climate change scenarios developed by the Ministry of Natural Resources and Environment (currently part of the Ministry of Agriculture and Environment), updated in 2020 (MoNRE, 2020). These scenarios are based on IPCC Fifth Assessment Report (AR5) projections under the RCP4.5 and RCP8.5 scenarios and provide detailed regional assessments for different parts of Vietnam. The choice of AR5 SLR projections while atmospheric variables are taken from AR6 reflects the availability of nationally downscaled and officially adopted SLR scenarios for Vietnam. Differences between AR5 and AR6 global mean SLR projections are minor before mid-century and exhibit limited scenario sensitivity prior to 2050, while uncertainties associated with ice-sheet dynamics dominate in both assessment cycles (Slangen et al., 2023; IPCC, 2023). Consequently, the combined use of AR5 SLR and CMIP6 climate projections is unlikely to introduce a significant bias in near- to mid-term impact estimates.

For Vietnam, SLR projections under RCP4.5 and RCP8.5 scenarios indicate a nearly linear increase in sea level through 2100 of about 54 cm (33–76 cm) and of about 73 cm (50–103 cm), respectively, compared to the baseline period of 1986–2005. To account for uncertainties arising from future global Greenhouse Gas (GHG) emissions and climate sensitivity in the timing of +2°C, +3°C, and +4°C GWLs and to represent a more extreme condition for the study area, this study adopts the RCP8.5 scenario. For each GWL, the corresponding SLR was estimated by linearly interpolating the RCP8.5 time series over the time window in which the warming level is reached in each GCM and SSP scenario.

2. Methods

The SWAT hydrological model has been extensively applied to simulate streamflow dynamics across diverse climatic scenarios and hydrologic response unit (HRU) configurations, while the HEC-RAS 2D hydraulic model is widely recognized for its effectiveness in riverine flood analysis. In this study, the complementary strengths of these two models were integrated to project flood depth, inundation extent, and flood hazard in the study area under future climate conditions. The conceptual framework for the coupled SWAT–HEC-RAS modelling approach employed in this research is presented in Figure 3.

Figure 3. Conceptual flowchart of the modeling framework to assess future flood hazards, considering the impacts of climate change, land use changes, and dam operation.

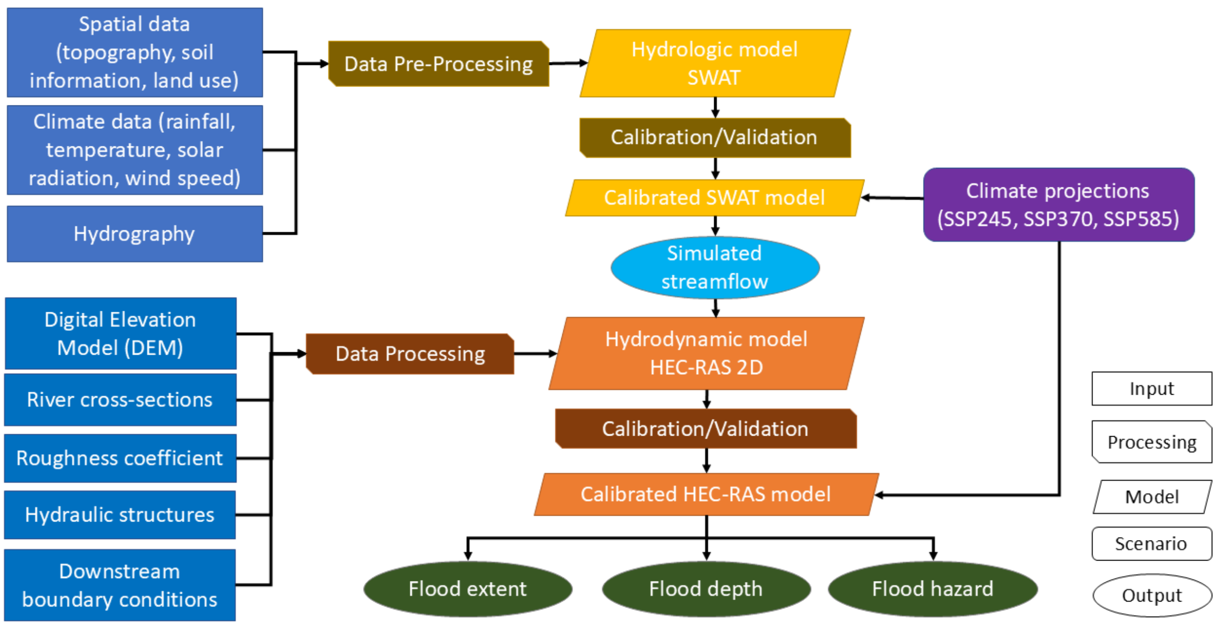

2.1. SWAT Model

The SWAT model, developed by the Agricultural Research Service of the U.S. Department of Agriculture (Gassman et al., 2007), is a process-based, semi-distributed, continuous-time hydrological model designed to assess the impacts of land-management practices on water resources and non-point source pollution in large river basins. Its application requires diverse datasets, including topographic, land-use, soil, and meteorological information, as well as multi-temporal observed streamflow records for model calibration and validation. The meteorological inputs typically comprise precipitation, air temperature, wind speed, solar radiation, and relative humidity. In this study, the SWAT modelling workflow began with watershed delineation using terrain data, followed by the subdivision of the basin into multiple sub-watersheds. Subsequently, hydrologic response units (HRUs) were defined based on the combination of land-use, soil, and slope characteristics.

The SWAT model is fundamentally governed by a water balance equation, which forms the basis of its hydrological computations. The specific formulation employed in SWAT is presented in Equation (1)

$$SW_t = SW_0 + \sum_{i=1}^{t}(R_{day} - Q_{surf} - E_a - W_{seep} - Q_{gw}) \quad (1)$$

where SW_t is the final soil water content (mm), SW_0 is the initial soil water content (mm), t is the elapsed time (days), R_{day} denotes daily precipitation (mm), Q_{surf} is surface runoff, E_a is evapotranspiration, W_{seep} represents daily seepage losses (mm), and Q_{gw} corresponds to daily groundwater return flow.

The generation of surface runoff is represented as a function of daily precipitation (R_{day}, mm) and the retention parameter (S, mm), following the empirical formulation of the Soil Conservation Service Curve Number (SCS-CN) method (SCS, 1972). The SCS-CN relationship is expressed in Equation (2).

$$Q_{surf} = \frac{(R_{day} - I_a)^2}{R_{day} - I_a + S} \quad (2)$$

where Q_{surf} denotes the daily surface runoff (mm), R_{day} is the daily precipitation depth (mm), and I_a represents the initial abstraction, defined as $I_a = 0.2S$ (mm). Parameter S, or the retention parameter, is not constant; rather, it varies according to factors such as slope, soil characteristics, and land-use management practices. Mathematically, the retention parameter S can be expressed as shown in Equation (3).

$$S = 254 \times \left(\frac{100}{CN} - 1\right) \quad (3)$$

where S denotes the retention parameter (mm) and CN is the curve number, which ranges from 0 to 100. A CN value of 100 indicates no potential retention, whereas a value of 0 corresponds to an infinitely large potential retention capacity.

2.2. HEC-RAS Model

The HEC-RAS model – developed by the U.S. Army Corps of Engineers (USACE, 2024) for one- and two-dimensional unsteady hydraulic simulations, sediment transport modelling, and water-quality assessments – is widely employed in research and practice. Although HEC-RAS offers a broad suite of modelling capabilities, this study focuses exclusively on two-dimensional flood-inundation modelling. The HEC-RAS 2D module solves either the Shallow Water Equations (SWE) or the simplified Diffusion Wave Equations (DWE) using an implicit finite-volume numerical scheme to simulate unsteady two-dimensional flow across computational meshes. These governing equations represent the conservation of mass and momentum, with the choice between SWE and DWE determining the level of hydrodynamic complexity—SWE retaining full momentum terms for more detailed flow representation.

The HEC-RAS model requires multiple input datasets, including terrain, land-use information, and unsteady discharge time series. In HEC-RAS, land use is used to assign Manning's roughness coefficients, which characterize surface resistance. The unsteady discharge generated by the SWAT model serves as the hydrological input for the hydraulic simulations. In the 2D flood module, the terrain is discretized into a computational mesh or grid that represents the land surface continuously, allowing water to propagate across the domain in both longitudinal and lateral directions.

2.3. Model Configuration

2.3.1. Hydrological model setup

The study area was delineated into 153 sub-watersheds and 2,580 hydrologic response units (HRUs) (Nguyen et al., 2024a, 2025d). Hydrometeorological data for the VGTB River basin are available for the period 1976–2023. Based on these datasets, the SWAT model configuration incorporated a 5-year warm-up period (1976–1980), followed by a 15-year calibration period (1981–1995). For model verification, the 28-year validation period was divided into two phases: a 15-year pre-dam period (1996–2010) and a 13-year post-dam period (2011–2023). The SWAT model was executed at a daily time step for both calibration and validation and subsequently used to simulate daily streamflow at the Thanh My and Nong Son stations, which serve as the upstream boundary conditions for the HEC-RAS hydrodynamic model.

The calibrated model was then used to simulate streamflow under historical climate (from 1980 to 2014) and future climate under SSP2-4.5, SSP3-7.0, and SSP5-8.5 (from 2015 to 2099) as simulated by CMIP6 GCMs. Note that these simulations also had a 5-year warming period, making historical simulations for streamflow available from 1985 to 2014, while projected streamflow is available from 2020 to 2099.

2.3.2. Hydrodynamic model setup

The flood maps in this study were generated using the HEC-RAS 2D model, driven by streamflow simulated by the SWAT model. A LiDAR-derived DEM with a spatial resolution of 5 m × 5 m served as the terrain input. The spatial extent of the HEC-RAS domain (highlighted in Figure 1b) differed from that of the SWAT model, as the analysis focused specifically on historically inundated areas identified from observed flood-trace maps. This downstream portion of the VGTB River basin is characterized by low-relief topography, in contrast to the predominantly mountainous terrain of the upstream area modelled by SWAT.

The Manning's roughness coefficients used in the HEC-RAS model were derived from the land-use/land-cover (LULC) map obtained from JAXA's High-Resolution Land Use and Land Cover dataset. For calibration purposes, the roughness values were categorized into normal, minimum, and maximum ranges. These parameter groups were subsequently employed in the calibration of the flood-inundation model.

2.3.3. Model Evaluation

A SWAT model must undergo three essential procedures, namely sensitivity analysis, calibration, and validation, before it can be reliably applied. During sensitivity analysis, statistical measures such as the *t*-value and *p*-value are used to evaluate the influence of individual parameters. A parameter is considered statistically significant when its *p*-value is less than 0.05, leading to rejection of the null hypothesis. In SWAT sensitivity analysis, parameters with large absolute *t*-statistics and low *p*-values were identified as highly sensitive, reflecting a strong influence on simulated streamflow.

The Pearson correlation coefficient (R), percent bias (PBIAS), Root Mean Squared Error (RMSE), RMSE–standard deviation ratio (RSR), and Kling–Gupta Efficiency (KGE) were employed to evaluate the model's daily discharge performance during both calibration and validation. The RSR, defined as the ratio of RMSE to the standard deviation of observed streamflow (Equation 4), ranges from 0 (optimal) to large positive values, with lower RSR and RMSE values indicating improved model performance. PBIAS measures the average tendency of simulated data to be larger or smaller than their observed counterparts (Equation 5), with values less than ±15% reflecting relatively good predictive skill. We also used the KGE metric (Equation 6) to measure model performance, which ranges from -∞ to 1, and values closer to 1 indicating superior model performance.

$$RSR = \frac{RMSE}{STDEV_{obs}} = \frac{\sum_{i=1}^{n}(O_i - S_i)^2}{\sum_{i=1}^{n}(O_i - \bar{O})^2} \quad (4)$$

$$PBIAS = \frac{\sum_{i=1}^{n}(O_i - S_i)}{\sum_{i=1}^{n}(O_i)} \quad (5)$$

$$KGE = 1 - \sqrt{(r-1)^2 + (\beta - 1)^2 + (\gamma - 1)^2} \quad (6)$$

where O_i and S_i denote the observed and simulated values, respectively; n is the number of paired observations; and $\bar{O}$ is the mean of the observed values. The term r represents the Pearson correlation coefficient, which characterizes errors related to the shape and timing of the hydrograph. The parameter β quantifies the bias between observed and simulated values, while γ is the ratio of the coefficients of variation of the simulated and observed datasets, describing variability-related errors while accounting for bias.

In hydrologic research, acceptable model performance is generally indicated by an NSE value greater than 0.50 and an RSR value less than 0.70. In addition, KGE values may be classified as follows: good (KGE ≥ 0.75), intermediate (0.75 > KGE ≥ 0.50), poor (0.50 > KGE > 0), and very poor (KGE ≤ 0).

Simulated and observed streamflow at the Thanh My and Nong Son stations were used to compute the evaluation metrics for the SWAT model, whereas simulated and observed water levels at the Cam Le, Cau Lau, Ai Nghia, and Giao Thuy stations were employed to assess the performance of the HEC-RAS model.

2.4. Estimation of flood magnitude using the Annual Exceeding Probability approach

This study used extreme streamflow simulated by the SWAT model as the upper boundary condition for the HEC-RAS simulation used to generate inundation maps. The extreme streamflows were calculated using the statistical methods outlined in Vietnamese Standard - Calculation of Design Hydrological Elements (TCVN 13615:2022). Specifically, the Generalised Extreme Value (GEV) distribution was used to determine the magnitude of streamflow corresponding to a specific Annual Exceeding Probability (AEP) as illustrated in Figure 4.

Figure 4. Conceptual flowchart for the estimation of flood magnitude using the Annual Exceeding Probability approach.

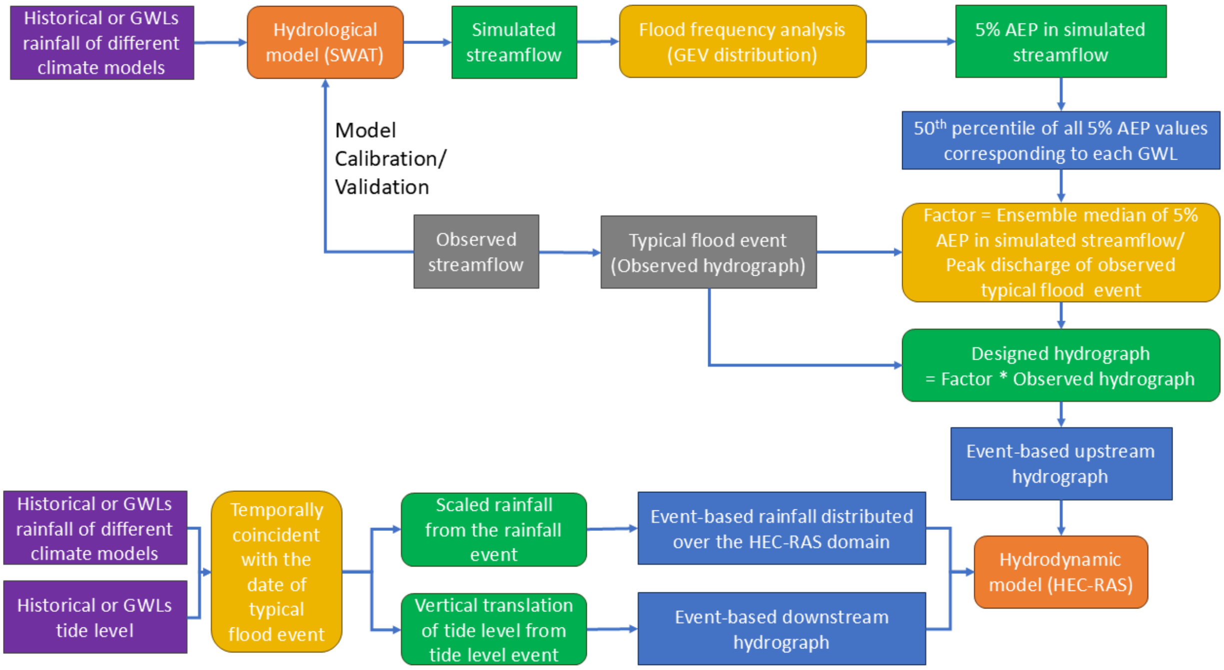

The 5% AEP (corresponding to a 20-year return period and usually recommended for hydraulic engineering design) was used to represent streamflow leading to floods. A typical flood event with peak discharge near the 5% AEP simulated streamflow was identified from the observed streamflow. Although multiple typical flood events could be selected for different 5% AEP simulations across the historical period (1995–2014) and under global warming levels (2, 3, and 4 °C), the 2020 flood event was adopted as a common baseline for all cases. This event was chosen because it is a recent, high-magnitude flood that captures the influence of upstream reservoir operations implemented after 2015. Furthermore, flood extent data from the 2020 event were used to validate the hydraulic inundation model.

We note that the 2020 flood was an extreme event of greater magnitude than a 5% Annual Exceedance Probability (AEP) flood. During this event, several reservoirs reached their maximum pool levels and were therefore no longer able to regulate streamflow dynamics as intended. To ensure that the inundation modelling reflected the conditions of a 5% AEP event, we used only the temporal pattern of the observed 2020 flood (i.e., the shape and timing of the observed flood hydrograph), while scaling the hydrograph magnitude to the simulated 5% AEP discharge for the historical period and for each future warming level, as illustrated in Figure 5. This approach ensured a consistent temporal structure across scenarios while allowing flood magnitude to vary according to the corresponding 5% AEP estimates. Nevertheless, the method assumes that the temporal pattern of the 2020 event is representative of future 5% AEP floods. This assumption may not fully capture differences in reservoir storage conditions or operational responses and should therefore be recognised as a limitation of the assessment.

Rainfall and tide levels coincident with the selected event were extracted from the climate forcing and tide datasets. Future climate rainfall was used to scale the baseline rainfall, while projected sea-level rise was added to the tide levels to generate event-based inputs. These were then applied as distributed rainfall over the HEC-RAS domain and as downstream boundary hydrographs for the model (Figure 4). This event-based selection ensured temporal and hydrological consistency between the prescribed upstream inflow hydrograph, the rainfall forcing, and downstream boundary conditions used in the hydrodynamic simulations.

Figure 4 illustrates the computational process used to identify upstream discharges for the flood events applied as boundary conditions in the HEC-RAS model:

- Observed daily streamflow at Thanh My and Nong Son stations (1976–2023) was used to calibrate and validate the SWAT model.
- The simulated historical streamflow was then subjected to flood frequency analysis to estimate the 5% AEP discharge. This threshold was used to identify a representative flood event in the observed record with a comparable peak discharge (for the historical period: flood event of 2020 was selected, dashed line in Figure 5).
- Climate forcing (daily temperature and precipitation) from 19 GCMs was used to drive the SWAT model to simulate streamflow and estimate the simulated 5% AEP discharge for the historical period (1995–2014) and at global warming levels of 2°C, 3°C, and 4 °C. The ensemble median of the simulated 5% AEP values was adopted to represent the discharge associated with a typical 20-year return period flood under historical and future warming conditions.
- A scaling factor was computed as the ratio between the ensemble median of simulated 5% AEP discharge for the historical period (1995–2014) and the peak discharge of the 2020 typical flood hydrograph. This factor was applied to the typical flood hydrograph to generate a scaled flood event, which served as the upstream boundary condition for historical flood inundation simulations (the black line in Figure 5). Hence, the hydrograph is defined as:

$$Q(t) = Q_{obs(2020)}(t) \times \frac{Q_{5\%}^{sim}}{Q_{peak,2020}^{obs}}$$

with $Q_{obs(2020)}(t)$ the observed hydrograph during the 2020 flood event, $Q_{5\%}^{sim}$ the ensemble median of the simulated 5% AEP streamflow and $Q_{peak,2020}^{obs}$the peak discharge of the 2020 flood event. Note that this approach assumes that climate change mainly affects the amplitude of the hydrograph, but note the shape.

Similarly, for future global warming scenarios, scaling factors were defined as the ratio of the ensemble median of simulated 5% AEP discharges under each GWL to the peak discharge of the 2020 typical flood hydrograph. These factors were applied to the typical 2020 flood hydrograph to generate scaled flood events (Figure 5), which served as upstream boundary conditions for the flood inundation simulations under future climate conditions.

Figure 5. Illustrations of observed typical flood event 2020 and scaled 5% AEP in simulated streamflow over the historical period (1995-2014) and for different GWLs at Thanh My station.

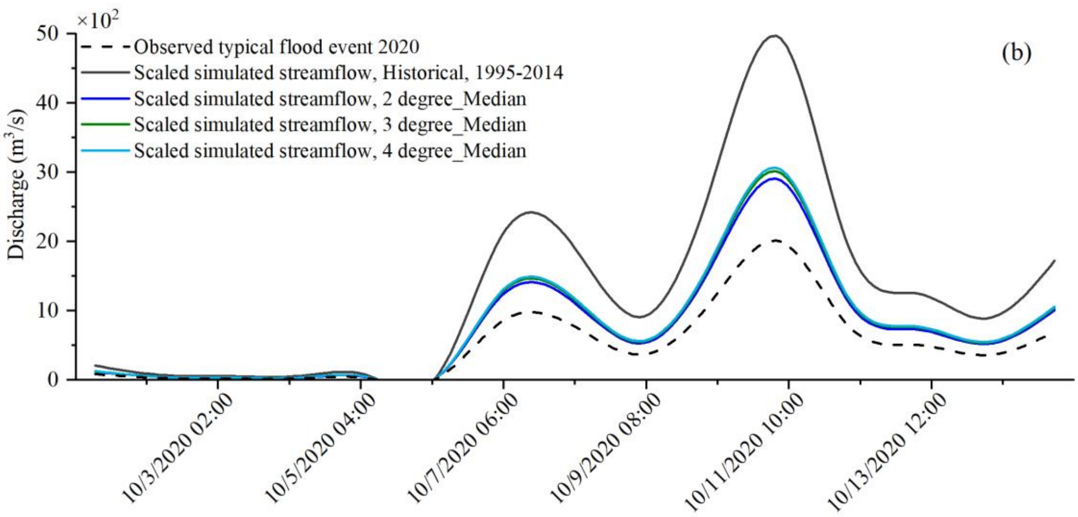

2.5. Assessing the impacts of climate change and human intervention on flood hazards

To provide a holistic perspective on potential drivers of changes in flood hazards, this study includes three inter-connected assessments to understand the influence of climate change and dams on streamflow regimes and flood inundation (see Figure 6). The first two experiments focus on the dynamics of river streamflow (which will then be used as the upper boundary for flood inundation modelling) modulated by climate change and human interventions, while the third experiment will focus on the dynamics of flood hazards (extents and depths). The following sub-section will provide more details on the approaches and methods adopted in the experiments.

Figure 6. Conceptual flowchart representing the steps taken to conduct three experiments that assess the impacts of climate change and human intervention on streamflow characteristics and flood hazards.

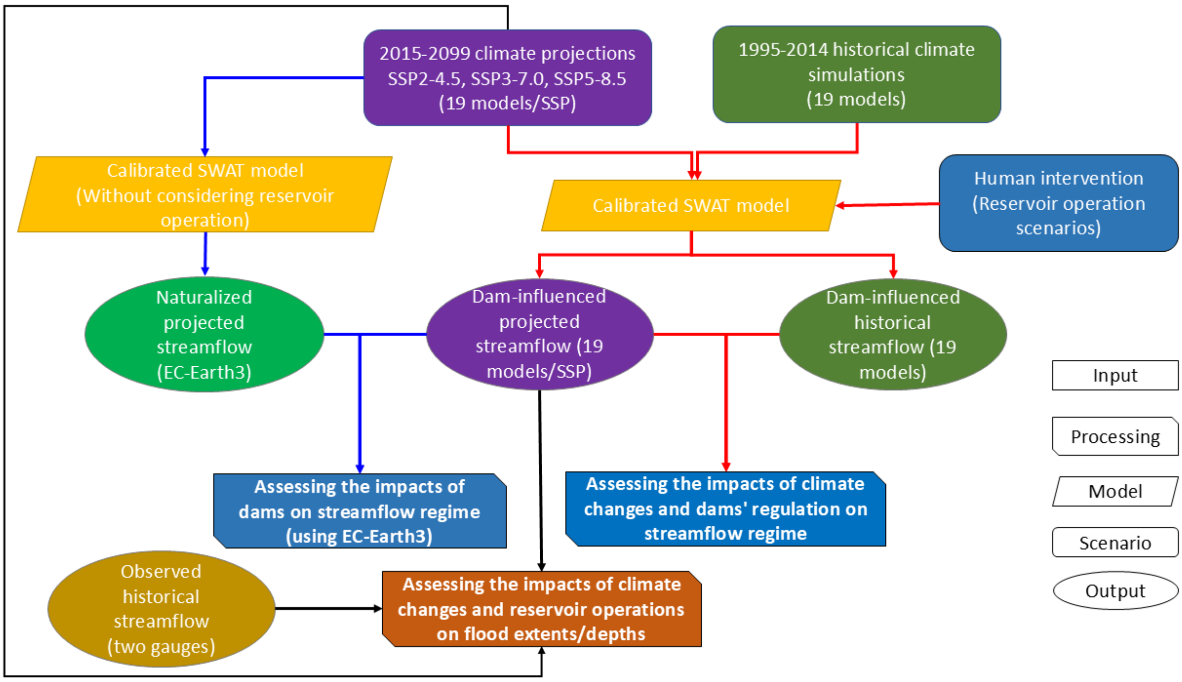

2.5.1. Quantifying the impacts of dams on streamflow regime

We first assessed how dams influence streamflow characteristics at two key hydrological stations (Nong Son and Thanh My) using the SWAT model. These simulations used the EC-Earth3 climate forcing and served as a control experiment in which reservoir operations are the only variable being manipulated, while other features of the hydrologic cycle remained the same. The EC-Earth3 model was selected as it shows relatively good performance over Vietnam (Nguyen-Duy et al., 2023) and also reaches most of the GWLs under the 3 SSPs (as shown in Table 3). Specifically, the SWAT model was customized to represent two scenarios of human intervention:

(i) The "dammed simulation": reservoir operation rules are included in the SWAT simulation.

(ii) The "naturalized simulation": all reservoirs are "muted" in the SWAT simulation.

The historical and future (under two reservoir scenarios) daily streamflow generated by the SWAT model was then assessed to see how streamflow characteristics have been influenced by reservoir operations. To connect changes in streamflow characteristics to future climate, we also focused on the time periods where EC-Earth3 reaches a global warming level (GWL) of +2°C, +3 °C, and +4°C, respectively, which are introduced in Table 3.

2.5.2. Quantifying the combined impacts of climate change and human intervention on streamflow regimes

In this assessment, the SWAT model (considering all reservoir operation rules) will be forced by (i) simulated historical climate and (ii) SSPs climate projections (under SSP2-4.5, SSP3-7.0, and SSP5-8.5) derived from the 19 GCMs listed in Table 3. By comparing future streamflow to historical simulated streamflow, we quantify changes in flow regimes under the influences of both climate change and reservoir operations.

Similar to the first experiments, we also focused on how streamflow will change under different GWLs. To achieve this objective, we used the information outlined in Table 3 and synthesized all streamflow values corresponding to a specific GWL, regardless of SSPs. The range of streamflow associated with a specific GWL was then compared with the range of streamflow simulated during the historical period (when forced by the same GCM). This approach is different from the conventional approach in climate impact assessment, where the future time window is usually pre-determined (e.g., using 2040–2059 and 2070–2099 as mid-century and end-century milestones) and the assessment is conducted separately for the selected SSPs.

2.5.3. Assessing the impacts of climate change and human intervention on future flood hazards

A similar technique was used to identify the upper boundary condition for flood events occurring under a specific global warming level. To take into account climate projection uncertainties, we used the following approach to identify – for each GWL – the "dry", "normal" and "wet" boundary conditions:

- **Step 1:** Identify all GCM-SSP simulations reaching each GWL. As illustrated in Table 1, there are 53, 46, and 21 GCM-SSP simulations available for GWL of 2°C, 3°C, and 4°C, respectively. Each GCM-SSP simulation provides a 20-year series of daily temperature and rainfall.

- **Step 2:** Run the SWAT model using the climate projections of each GCM-SSP simulation, to obtain 20-year series of daily streamflow.

- **Step 3:** Compute the annual maxima (AMAX) values of streamflow simulated at Nong Son and Thanh My stations for each GCM-SSP simulation.

- **Step 4:** Compute the 5% AEP values corresponding to a specific GCM-SSP simulation (from the 20-year AMAX time series obtained from step 3), using the GEV approach (see Section 2.4).

- **Step 5**: Estimate the values corresponding to the 25th, 50th, and 75th percentiles of all available 5% AEP values corresponding to a specific GWL (e.g., 53 values for 2°C of GWL). The calculated percentiles were then used to represent the upper streamflow boundary of three different scenarios of a specific GWL: dry (25th percentile), modest (50th percentile), and wet (75th percentile).

- **Step 6**: Scale the typical flood event from the observed streamflow record to each scenario of a specific GWL identified in Step 5. The approach is similar to that described in Section 2.4: the ratios between the ensemble 25-/50-/75-th percentile of 5% AEP projected streamflow (calculated from step 5) and the peak discharge of observed typical flood hydrograph were computed, then served to scale hourly data of recorded flood events to yield the upper streamflow boundary condition for future flood inundation assessment.

Figure 7. Conceptual flowchart of the steps taken to assess the impacts of climate change and human intervention on flood depths and extents under different GWLs.

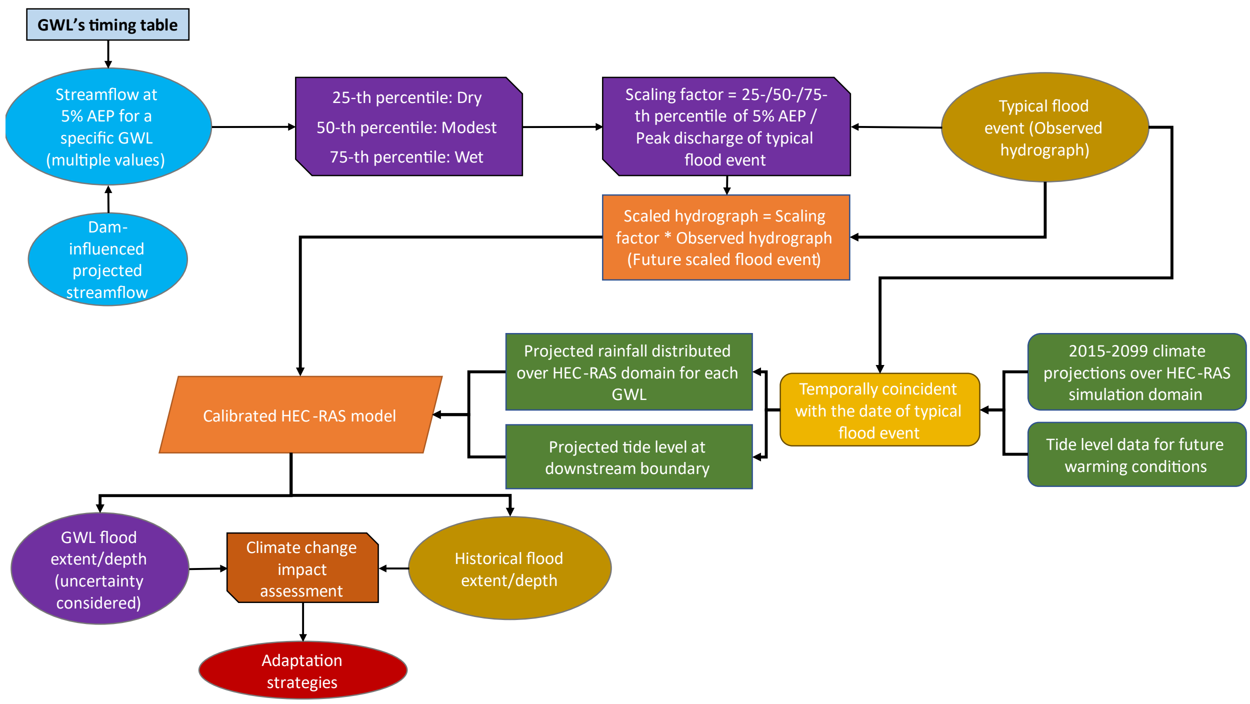

We also calculated extreme rainfall over the hydrodynamic simulation domain to replicate typical flood conditions in this area. Specifically, we calculated the average rainfall over the HEC-RAS domain and adopted the same procedure as for streamflow to identify 5% AEP rainfall of three different conditions (dry, modest, wet) corresponding to a specific GWL. In addition, the future state of tidal dynamics (the lower boundary condition in HEC-RAS) was also estimated using linear interpolation based on the mean values from scenarios for Vietnam that were made publicly available (see Section 1.4). The extents and depths under three different future states (dry, modest, wet) of a specific GWL were then compared with the historical flood hazard to guide policy recommendations.

3. Results

3.1. Observed changes in hydro-climatic variables across the Vu Gia Thu Bon River basin

We first investigate the changes in hydro-climatic variables (temperature, rainfall, and river streamflow) observed at the gauging stations across the river basin from 1980 to 2023. Figure 8 shows the results of this analysis (using a 20-year backward-moving window to highlight notable trends), demonstrating a steady rise in temperature indices (panels a and b) across three meteorological stations (see also Figure A.4). Over this 34-year period, the average temperature has risen by more than 0.5 °C, with the highest rate at Tra My station (an increase of 0.9 °C, reaching 25.3 °C at the end of the reference period in 2014).

Rainfall indices (panels c and d of Figure 8) show a general increasing trend over the recorded period, but the inter-annual variability is more complex, featuring a mild decline in the 2010s followed by a substantial increase since 2019. The high interannual variability hinders the reliable identification of significant trends over a time interval limited to a few years (see also Fig.A.4 for more information). Specifically, the median value of the 5%AEP rainfall (calculated from data available from 16 rain gauges) reached its lowest 20-year average value (389 mm) in 2019 before rising to its peak (452 mm) in 2023. By contrast, the evolution of river average streamflow at the hydrologic stations shows a clear increasing trend until about 2010, followed by a decreasing trend over the following years (except for 5% AEP streamflow at Nong Son). This pattern is particularly transparent at Thanh My station (representing streamflow of the Vu Gia River): both SOND (standing for September, October, November, and December) and 5% AEP streamflow indices exhibit a clear decreasing trend since 2010, reaching their lowest values (219 m^3/s for SOND streamflow and 8,797 m^3/s for 5% AEP streamflow) by the end of the reference period. This feature demonstrates the importance of the cascade of dams across the mainstem (fully operated since 2020, as demonstrated in Table A2 in the supplementary) on the streamflow regimes, which will be assessed in more detail in the following sections. Note that the apparent discrepancy between the absence of a rainfall trend and the increase in streamflow likely reflects the spatial variability of precipitation and the different sampling areas, with most meteorological stations located downstream, whereas hydrological stations integrate runoff from upstream.

Figure 8. Changes in temperature (a–b), rainfall (c–d), and river streamflow (e–f) indices calculated from data records at the hydro-climatic gauging stations across the river basin.

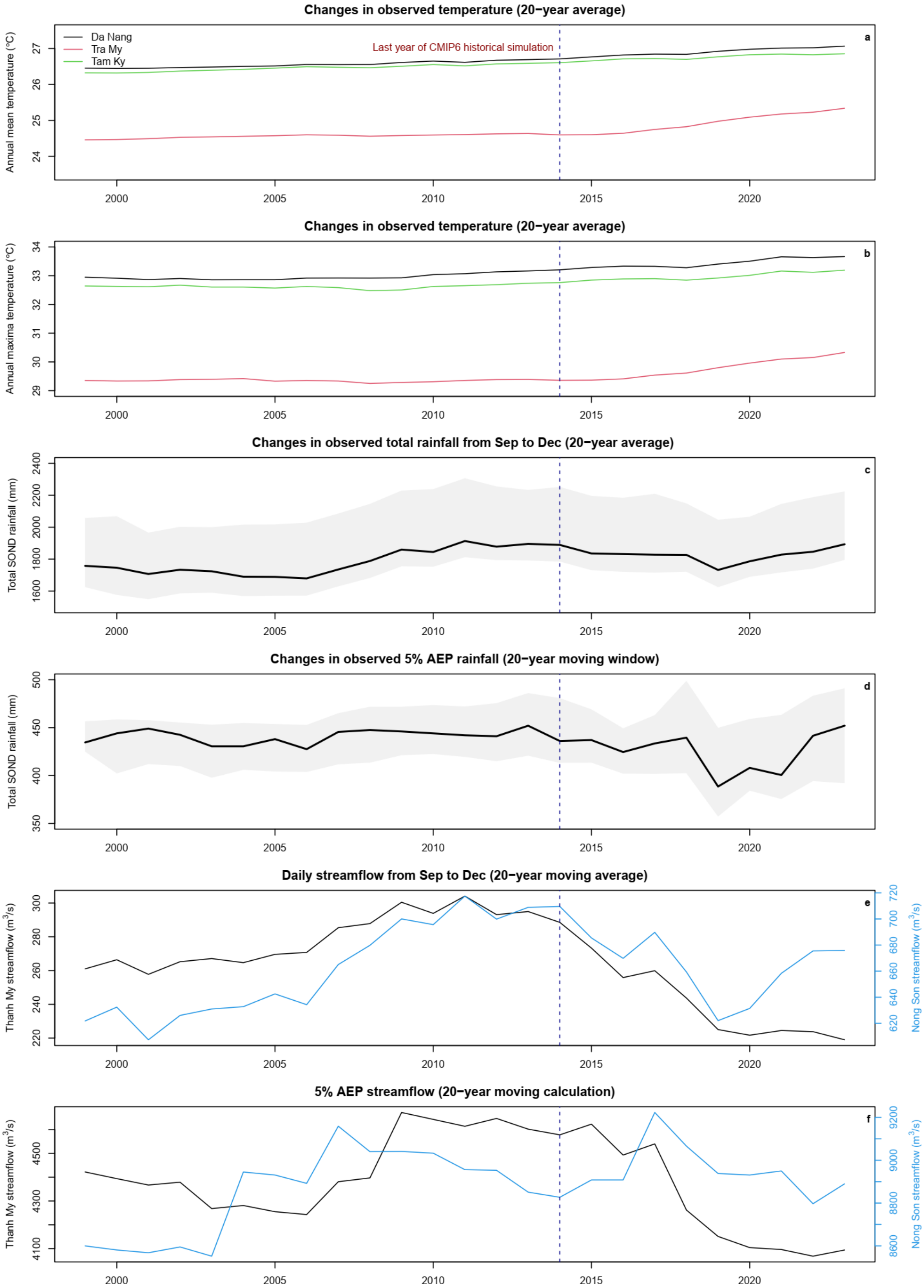

Note: A 20-year moving window was applied to highlight key trends over the observed period. The grey area and black line in panels c and d represent the 25th – 75th range and the median values calculated from data available at 16 rain gauges. The vertical dashed line marks the last year of the historical simulations as defined in this study.

3.2. Changes in simulated rainfall characteristics over the hydraulic simulation domain

We first assessed the dynamics of rainfall (the dominant driver of floods in Vietnam) using historical simulations from the climate models over the study area. Figure 9 illustrates changes in total rainfall over the flood season (from September to December; denoted as SOND rainfall) and the 5% AEP rainfall (representing extreme rainfall intensity that could lead to floods) over the HEC-RAS simulation domain (used as input in flood inundation simulation) under three selected emission scenarios (SSP2-4.5, SSP3-7.0, and SSP5-8.5). The SOND rainfall was first calculated separately for each year, and then a 20-year moving average technique (backwards-looking) was applied to highlight the overall trend (Figure 9a). The medians and the 25–75th percentile ranges were calculated using the results obtained from the 19 GCMs. We also calculated the Rx1day (the highest intensity of 1-day rainfall) for each year, then applied a 20-year moving window (backwards looking) to estimate the value corresponding to a 5% AEP (Figure 9c) as previously described in section 2.4.

Over the historical period (from 1980 to 2014), the general rainfall trend across the 19 GCMs is decreasing, although the rate of change is less notable in extreme rainfall than in the SOND rainfall. The discrepancy between observed and simulated precipitation trends can be attributed to 2 main factors: remaining biases in GCM outputs and the influence of the relatively short period (20 years) in a context of high interannual precipitation variability. In addition, the simulated total rainfall over SOND also appears significantly lower than observations, for which the 75th percentile reached about 2200 mm in the 2010s. By contrast, simulated 5% AEP values are in the range of observations (Fig.9). In contrast, future rainfall generally exhibits an increasing trend for both SOND and extreme rainfall, regardless of emission scenarios. It is important to note that the intermodel variability is quite large, and the range between the 25th and 75th percentiles of SOND (5% AEP) rainfall estimated from the 19 GCMs can be up to 450mm (300mm). The trend in rainfall is also not linearly correlated to emission scenarios, as the SSP2-4.5 generally exhibited a higher intensity of rainfall throughout the rest of the 21st century relative to that simulated under the SSP3-7.0 scenario. Nevertheless, the SSP5-8.5 remains the scenario with the highest rainfall intensity, indicating that a high-emission scenario will potentially lead to more severe flood-inducing rainfall in the study area.

Figure 9. Evolution of total rainfall from September to December (SOND rainfall) (a) and the 5% AEP rainfall (c) over the 2D simulation domain between 2015 and 2100 under the three selected SSP scenarios, as simulated by the downscaled CMIP6 climate models. The boxplots (b and d) show the distribution of these time series (i.e., SOND and 5% AEP rainfall) to highlight key differences across scenarios.

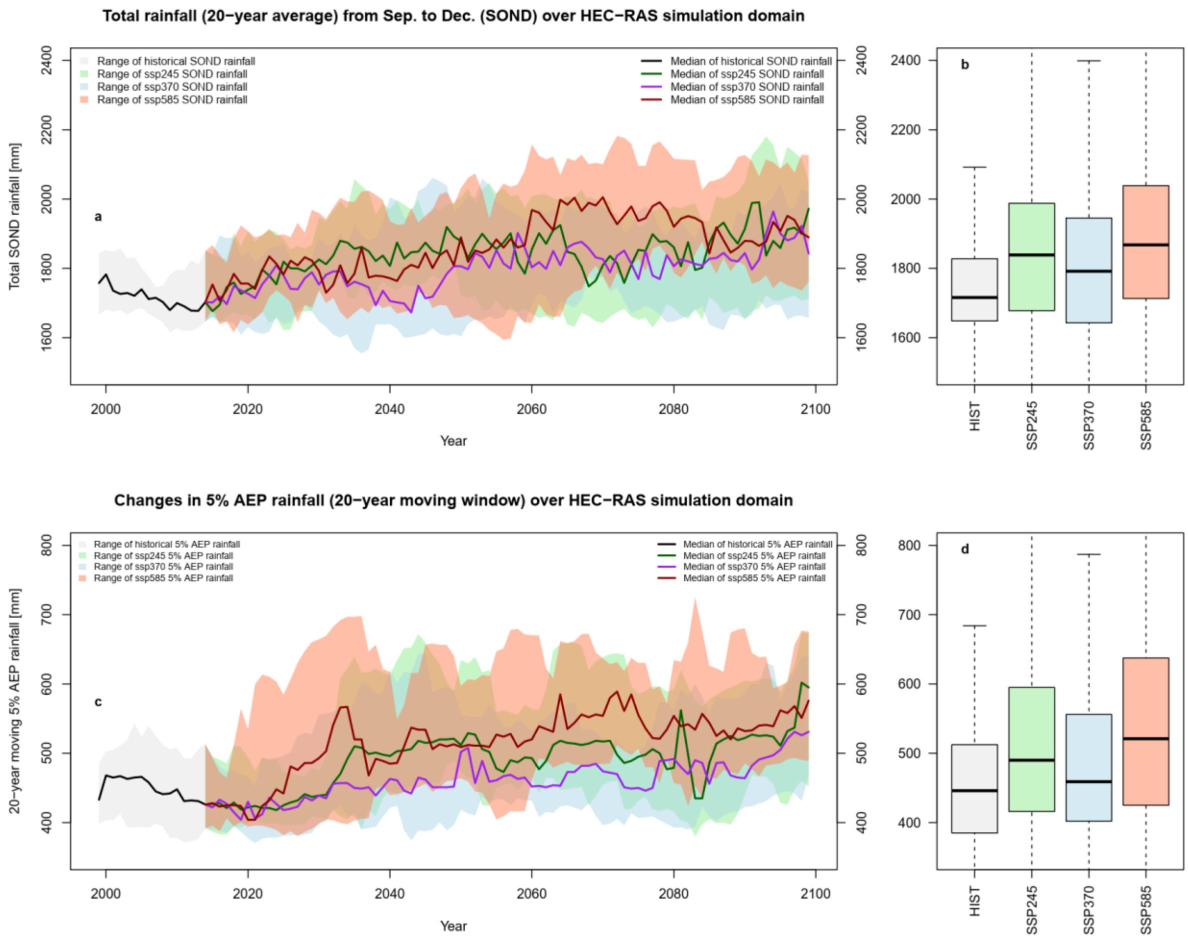

Figure 9 also highlights an important point for subsequent analyses, as reference period choice might lead to different findings. For instance, SSP2-4.5 generally yields a higher extreme rainfall intensity over the mid-century relative to the 2060-2080 period. In contrast, SSP5-8.5 introduces the highest extreme rainfall intensity over the 2060-2080 period, compared to the rest of the simulation timeframe.

3.3. Changes in river streamflow across different scenarios

3.3.1. Assessment of the hydrologic model capacity

Figure 10 compares simulated and observed streamflow time series for the SWAT model calibration and validation at the Thanh My and Nong Son stations. Model performance was quantitatively assessed using five efficient metrics (Table 4), which collectively indicate a satisfactory agreement between simulated and observed flows. During the first validation period, the Pearson correlation coefficient (R), Kling Gupta efficiency (KGE), ratio of the root mean square error to the standard deviation of observations (RSR), root mean square error (RMSE), and percent bias (PBIAS) at the Thanh My station were 0.88, 0.79, 0.53, 142.12 m^3/s, and -12.38%, respectively. Corresponding values at the Nong Son station were 0.90, 0.78, 0.44, 305.29 m^3/s, and 1.83%.

Figure 10. Observed and simulated daily streamflow at (a) Thanh My and (b) Nong Son stations.

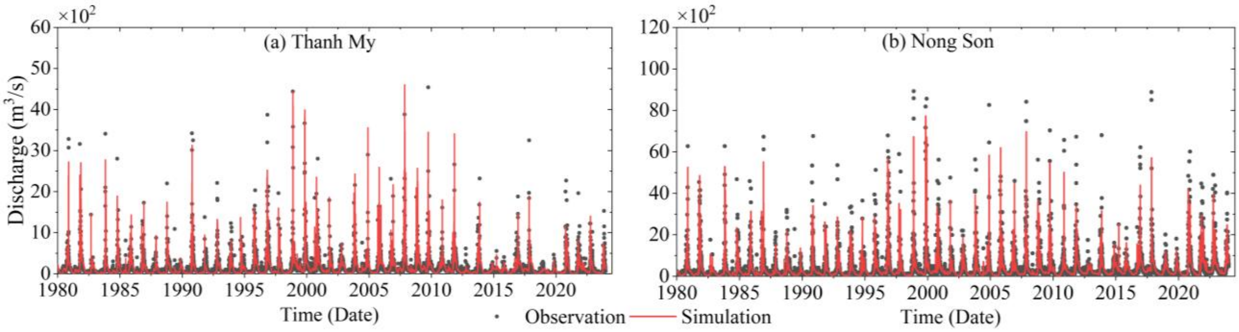

Similar levels of agreement were obtained in the second validation period, demonstrating the robustness of the model across different hydrological conditions. Although flood peak values differ across years, the results confirm that the model setup can be used to assess the impacts of climate change and upstream dam development on streamflow.

Table 4. Performance of the SWAT model for calibration and validation at two hydrological stations.

Statistical indices	Thanh My station (Vu Gia River)			Nong Son station (Thu Bon River)		
	Calibrated (1980–1995)	First Validated (1996–2010)	Second validated (2011–2023)	Calibrated (1980–1995)	First Validated (1996–2010)	Second validated (2011–2023)
R	0.82	0.88	0.82	0.90	0.90	0.91
KGE	0.82	0.79	0.64	0.79	0.78	0.71
RSR	0.58	0.53	0.59	0.44	0.44	0.45
RMSE (m^3/s)	119.61	142.12	105.47	214.28	305.29	250.84
PBIAS	3.76	-12.38	-28.29	2.28	1.83	-5.68

3.3.2. The impacts of dams on river streamflow

This section assesses the impacts of dams on river streamflow, using streamflow simulated by the SWAT model under two future scenarios: (i) streamflow is not influenced by reservoir operations (the naturalized simulation) and (ii) streamflow is heavily modulated by reservoir operations (the dammed simulation). Climate outputs of the EC-Earth3 climate model were used identically to represent the historical climate as well as the future climate dynamics.

Figure 11. Seasonal streamflow variations under the historical and SSP2-4.5 (a), and SSP5-8.5 (b) emission scenarios as simulated by the SWAT model forced by climate projections of the EC-Earth3 climate model.

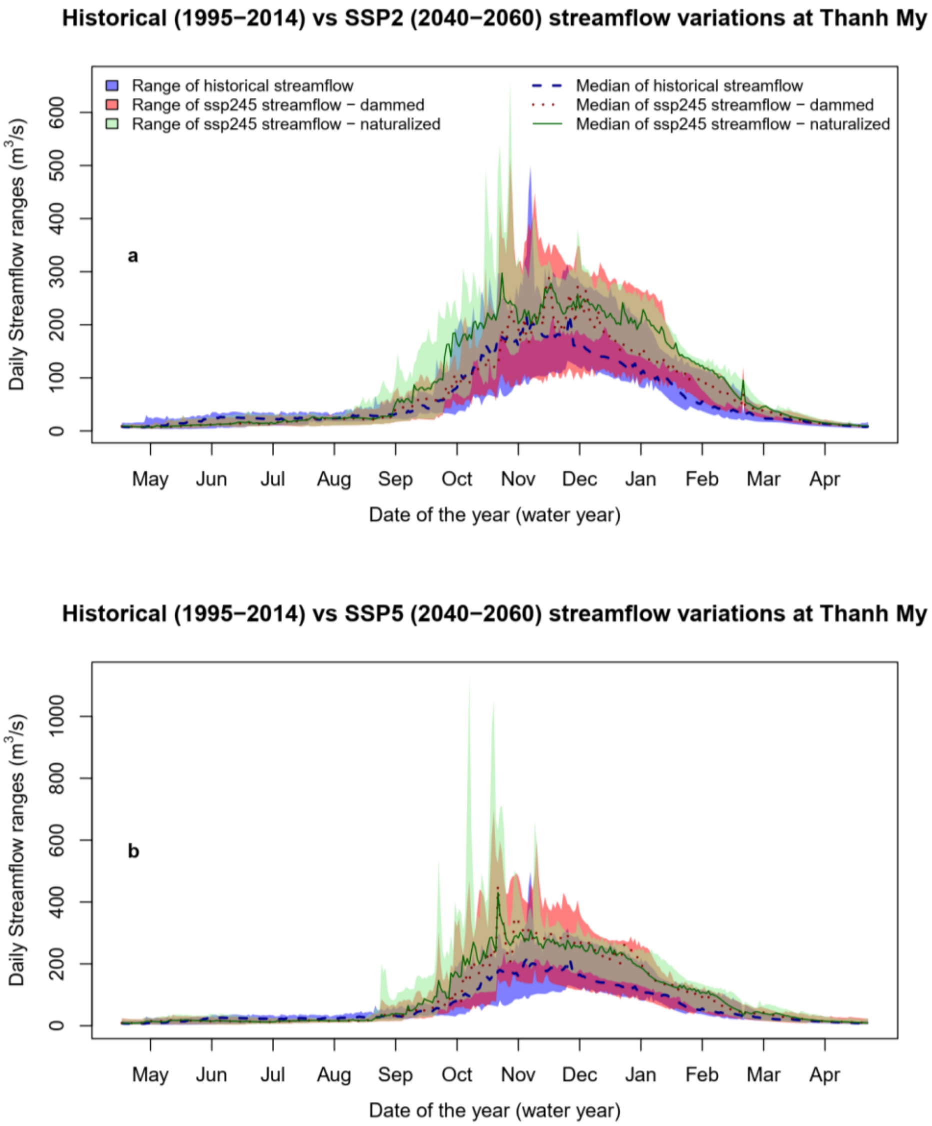

Note : Due to the transparent plotting option, some regions appear in colours different from those listed in the legend.

The SWAT model was forced by climate variables produced by EC-Earth3 climate models over the historical period (1995–2014; in blue) and mid-century period (2040–2059). The naturalized (dammed) simulations are highlighted in green (red) colors. The medians and the 25–75th percentile ranges were calculated for each day of the water year (from May of the current year to April of the next year) using the corresponding 20-year period.

We first examined changes in the seasonal hydrologic cycle at the VGTB river in the mid-century period (from 2040 to 2059) relative to the historical period (from 1995 to 2014). Figure 11 illustrates the results exhibited at Thanh My stations for the SSP2-4.5 (Figure 11.a) and SSP5-8.5 (Figure 11.b) scenarios. Both demonstrate a similar pattern to that exhibited in the SSP3-7.0 emission scenario as well as at the Nong Son hydrologic stations (not shown).

Overall, the range of future streamflow is generally higher than the historical period, regardless of human intervention scenarios. The increase in streamflow magnitude is particularly pronounced during extreme events, and the magnitude is higher in the SSP5-8.5 (higher than 1000 m^3/s) relative to the SSP2-4.5 emission scenario. Reservoirs also have a substantial impact on the streamflow seasonal cycle: the SOND streamflow has been reduced substantially (about 20% and 6% for SSP2 and SSP5 emission scenarios, respectively) as the reservoirs store water for later hydropower production. The magnitude of streamflow simulated in the dammed simulation is also significantly lower than that in the naturalized one, confirming the fact that dam regulations could reduce the potential flood hazards.

Figure 12 further highlights the impacts of reservoirs on streamflow regimes, showing a substantial increase in the projected annual mean streamflow at the Thanh My station compared to the historical simulation. Specifically, the range of historical streamflow (blue line) is generally between 50 and 200 m^3/s, indicating considerable inter-annual variability across the assessed period. In contrast, the future projections (2020–2100), simulated under three Shared Socioeconomic Pathways (SSP2, SSP3, SSP5), generally project a higher baseline streamflow, with annual values frequently reaching or exceeding 200 m^3/s, and spiking above 300 m^3/s in several instances. The dam-regulated simulations (red lines), however, demonstrate a substantially lower streamflow magnitude relative to the naturalized simulations (green lines), indicating that current operations tend to heavily regulate the natural variability of streamflow, leading to a reduced average streamflow in projected flow regimes. Furthermore, while all scenarios show high variability, there is no statistically significant trend (through a Mann-Kendall test at the 5% significant level) of monotonic increasing or decreasing mean streamflow over time, or as the global warming level (GWL) increases from 2°C (GWL2) to 4°C (GWL4) under the SSP5-8.5 scenario.

Figure 12. Annual mean streamflow calculated from the historical simulation (blue line) and the future simulations with dam regulation settings (red lines) as well as naturalized settings (green lines) under three emission scenarios at Thanh My station.

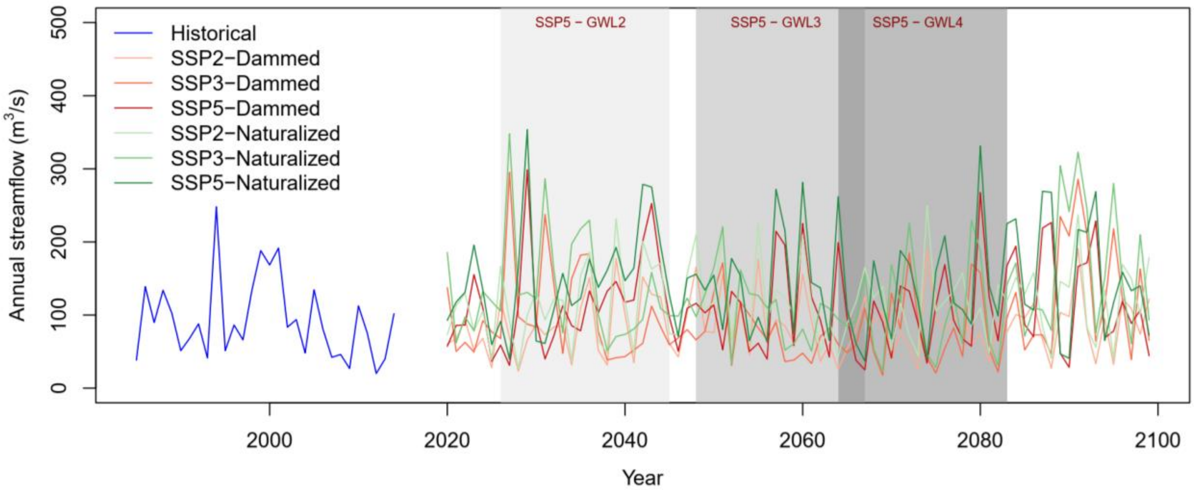

Note: The grey zone indicates the timing at which EC-Earth3 reaches a specific global warming level under the SSP5-8.5 emission scenario (GWL2, GWL3, and GWL4, respectively, denote a global warming level of 2-, 3-, and 4-degrees).

Figure 13 further complements the time series assessment by illustrating the distribution and range of annual and wet-season average streamflow, categorized by historical period and the three GWLs under dammed and naturalized conditions. The median annual streamflow for the historical period is approximately 75 m^3/s, generally lower than the streamflow magnitudes across all future scenarios (regardless of GWLs and whether reservoir operations are taken into account), with the median values between 100 m^3/s and 125 m^3/s. Across all GWLs, the dammed streamflow (red boxes) consistently shows a lower median value and a more constrained range, with a median value close to the historical one, further demonstrating the impacts of reservoirs. The assessment of wet-season average streamflow (Figure 13.b) highlights a similar message: no clear trend at higher GWL and dams have effectively offset the CC effect on flood season flows. Specifically, the historical median is consistently lower than natural values for all GWL, while the dammed simulation show similar median values (especially for GWL3 and GWL4). It is important to note that the naturalized GWL2 scenario generally projects the highest median flow (about 250 m^3/s), further confirming that there is no clear trend of increasing or decreasing in wet-season streamflow as the GWL increases from GWL2 to GWL4.

Figure 13. Boxplots showing the range of (a) simulated annual average streamflow and (b) wet-season average streamflow (calculated using daily streamflow from September to March the next year) for the historical (blue) as well as for future periods corresponding to three GWLs (+2-/3-/4-°C) using dammed (red boxes) and naturalized (green boxes) models at Thanh My station.

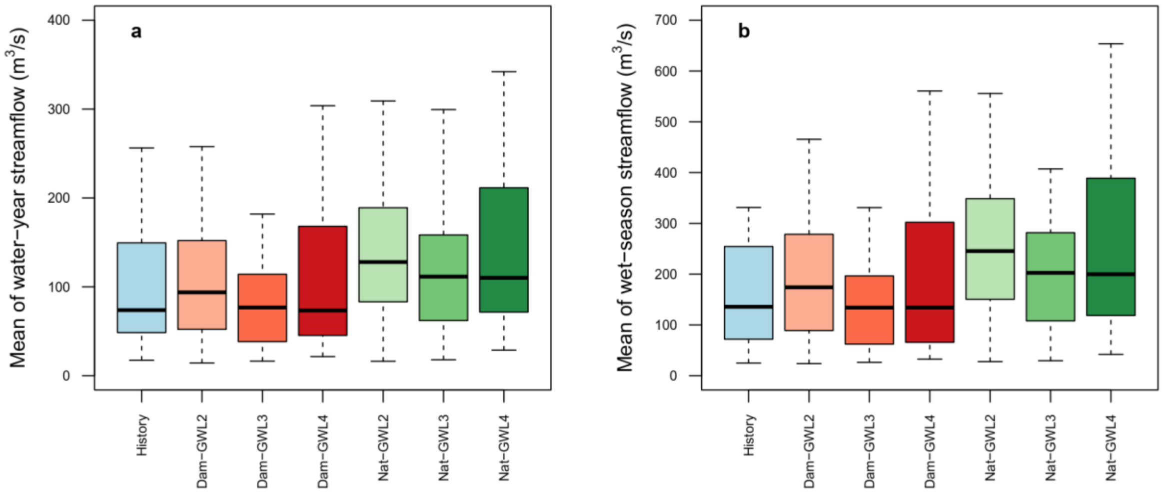

3.3.3. The combined impacts of climate change and dam regulations on river streamflow

Figure 14 shows changes in flood season streamflow (SOND) and extreme high flows (5% AEP) simulated by the SWAT model forced with CMIP6-VN data at two hydrological stations (Thanh My and Nong Son). To highlight the trend, the time series is smoothed using a 20-year moving average. We note that the historical (resp. future) simulation is available from 1985 to 2014 (resp. from 2020 to 2099), resulting in the 20-year moving average time series only available from 2004 to 2014 (resp. 2039 to 2099) for this assessment.

The most important pattern exhibited across both stations is a downward trend across the historical period, more pronounced at Thanh My station. We note that the inter-annual variability shows some discrepancies relative to that observed at the streamflow gauges (shown in Figure 9), owing to the uncertainty of rainfall pattern introduced through GCMs outputs (i.e., the CMIP6-VN data). The operations of hydropower reservoirs across the Vu Gia Thu Bon River Basin since the end of the 2000s (see Table A1 in the Appendix for more information) have altered the basin hydrological response to rainfall, and further reduced flood season streamflow as they need to store water to support hydropower production in the dry season. The pattern exhibited by extreme high flows (5% AEP) is more complex, with no clear distinction between the increase exhibited under the SSP2-4.5 and SSP5-8.5 emission scenarios at both stations. The projections indicate limited changes in average flood season streamflow (Figure 14a-b), except under SSP5-8.5. Over the 2039-2099 period, median SOND streamflow projection at Thanh My station shows no clear increase under SSP2-4.5, SSP3-7.0 (the rate of change – determined by Sen's slope – is 0%, 3.3% for the whole period), while SSP5-8.5 shows a small increase of 16%. Similar patterns are also observed in the 5% AEP streamflow, with the rate of changes over the entire period (determined by Sen's slope) is 4.5%, -0.2%, and 10.9% for SSP2-4.5, SSP3-7.0, and SSP5-8.5, respectively. The Mann-Kendall test at the 5% significance level further confirms these patterns, as the trend is only statistically significant for streamflow indices simulated under the SSP5 scenario. It is important to note that the increase in streamflow across the future projections over the Vu Gia River (represented by simulated streamflow at Thanh My station) is overshadowed by the influence of reservoir operation, as the magnitude of both the average flood-season and extreme streamflow is substantially lower than that exhibited over the historical period (by about 20% and 50% for SOND and 5% AEP streamflow respectively).

Figure 15 provides a more detailed assessment of the distribution of future SOND streamflow across different GWLs at Thanh My station, for each GCM used in this study. For the majority of simulated streamflow, the median SOND streamflow projected for all three Global Warming Levels (GWL2, GWL3, GWL4) is generally lower than the historical median, further confirming the impact of reservoir operations on flood season streamflow in a warming climate. The multi-model analyses also demonstrate a low, consistent relationship between the magnitude of flood streamflow and the degree of warming. This non-linearity at different GWLs can be attributed to the high inter-annual variability of rainfall simulated by the individual model (as shown in Figure 10), while the sampling period (20 years) is relatively short, which may significantly affect the results. For instance, ACCESS-ESM1-5, BCC-CSM2-MR, and FGOALS-g3 project a general increase in median flow from GWL2 to GWL4, while AWI-CM-1-1-MR and CNRM-CM6-1-HR show a decrease in median flow between GWL2 and GWL3, followed by an increase at GWL4, introducing significant uncertainty in the projections. Only a few of the climate models drive increased SOND streamflow at Thanh My station, with much higher extreme values at GWL3 or GWL4.

Figure 14. Changes in average daily streamflow from September to December (SOND) at (a) Thanh My station, (b) Nong Son station, as well as changes in 5% AEP streamflow estimated at (c) Thanh My station, (d) Nong Son station.

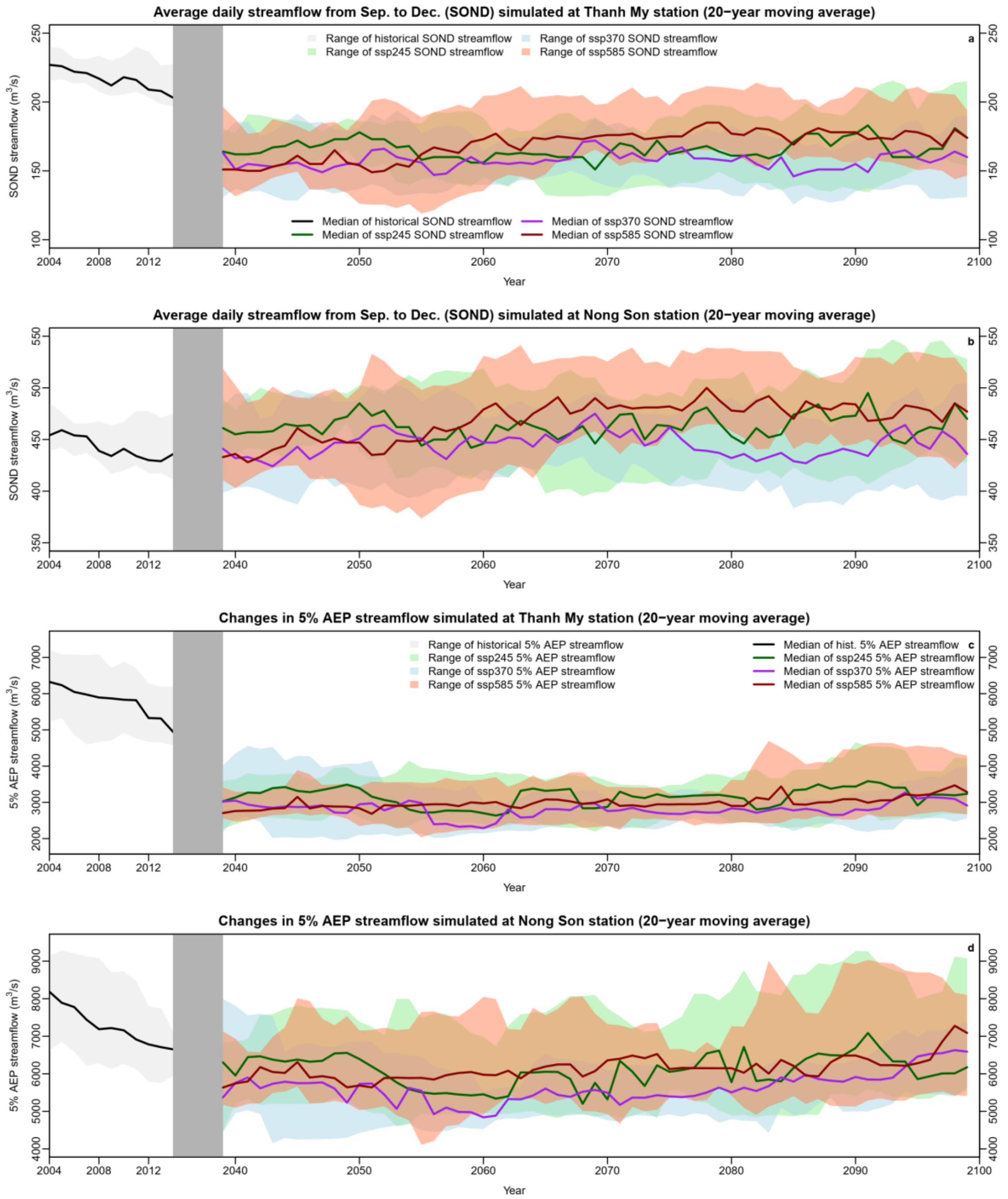

Note: Streamflow was simulated for the historical (1985–2014) and future (2020–2099) periods by the SWAT model forced with CMIP6-VN data. A 20-year backward-moving window was used to smooth the SOND streamflow and generate the 5% AEP time series. Note that the x-axis is not to scale between 2014 and 2039 (dark grey zone on the figures).

Figure 15. Boxplots showing the range of SOND historical and projected streamflow simulated at each GWLs (+2-/3-/4-degree) at Thanh My station. Each panel illustrates the results obtained from streamflow simulations forced with historical and projected climate outputs of a specific GCM.

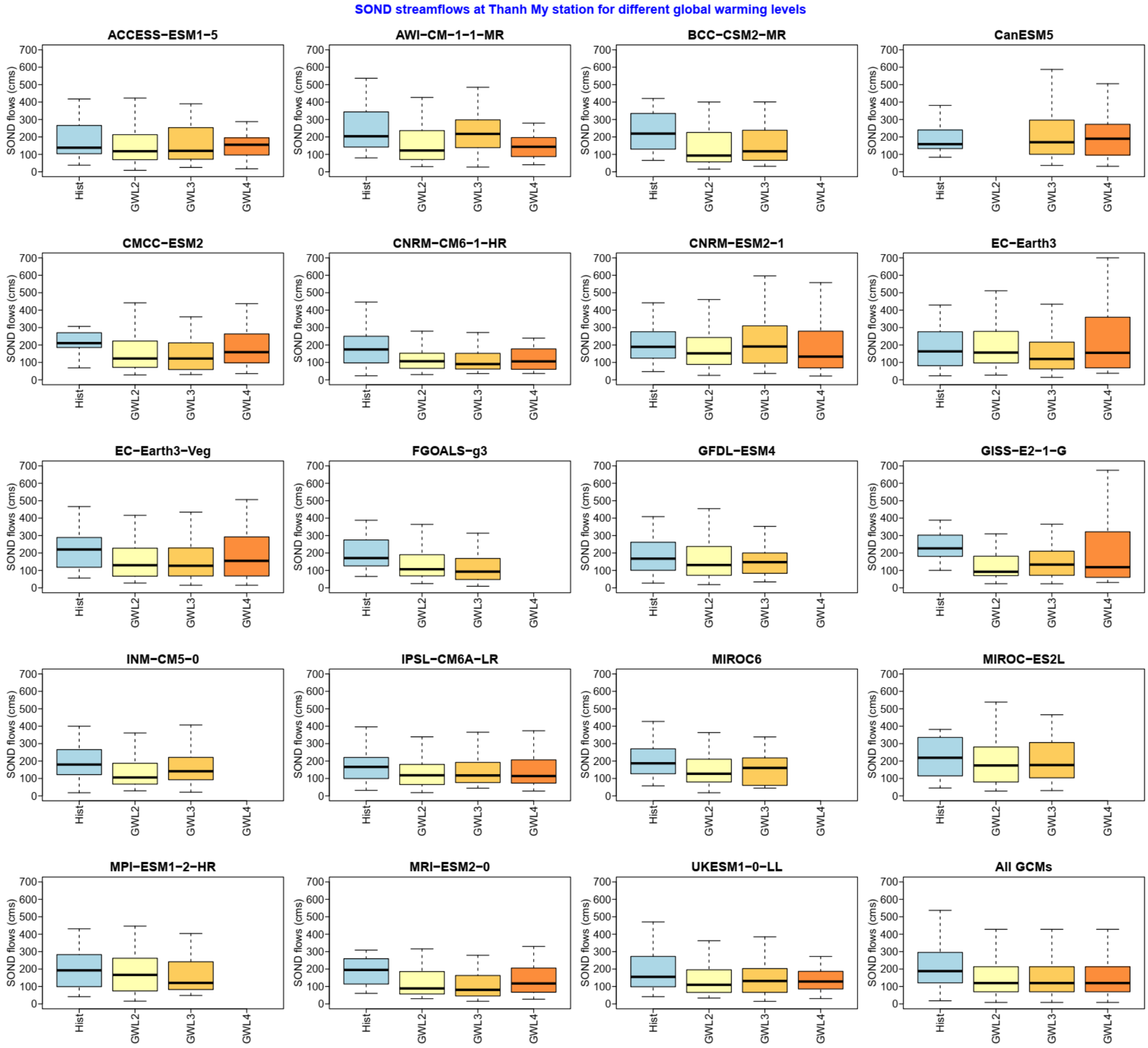

3.4. Projections of flood inundation

3.4.1. HEC-RAS model evaluation

The HEC-RAS model was calibrated and validated using the 2020 flood event (01–15 October), one of the most severe floods in the study basin, and well-suited to the available data collection period for simulation. A 10-day warm-up period (21–30 September) was applied to reduce initial-condition effects. Figure 16 compares observed and simulated hourly water levels at four hydrological stations along the VGTB River system (Ai Nghia and Cam Le stations along the Vu Gia River, Giao Thuy and Cau Lau along the Thu Bon River).

Observed water levels are shown as black lines, and simulated values as blue lines. The simulated hydrographs closely reproduce observed flood dynamics, including peak stages and temporal variability. NSE value exceeds 0.7 at all stations, indicating relatively good performance. These results confirm that the HEC-RAS model meets established hydrological performance benchmarks and reliably simulates flood water levels across different phases of the 2020 event.

Figure 16. Water level calibration results for the October 2020 flood at four representative hydrological stations: Ai Nghia and Cam Le on the Vu Gia River, and Giao Thuy and Cau Lau on the Thu Bon River.

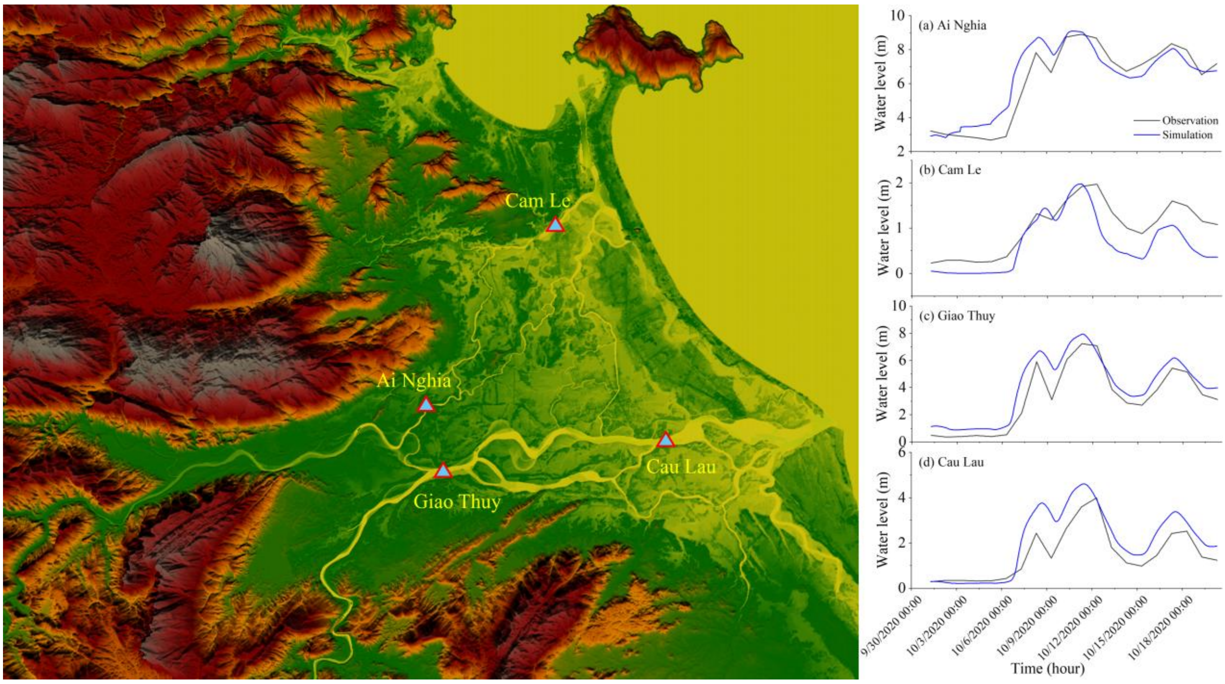

3.4.2. Future boundary conditions and scaling factors for flood inundation assessment

This section explores the combined effects of upstream dam development (all 18 major dams have fully functioned since 2020, as shown in Table A2, and no major dams are planned for the near future) and projected GWLs of 2°C, 3°C, and 4 °C on flood inundation patterns within the basin and maximum water levels at key hydrological stations along the VGTB River system. Figure 17 summarizes the simulated responses across four scenarios, including flow discharge at two representative stations—Thanh My on the Vu Gia River and Nong Son on the Thu Bon River (Figure 18.a), rainfall over the simulation domain (Figure 17.c), and ratios of peak values for each scenario relative to the 2020 flood event (Table 5).

Figure 17. (a)–(b) Observed flow discharge (m³/s) during the 2020 flood event and simulated flow for historical period and future periods at two main sites, Thanh My on the Vu Gia River and Nong Son on the Thu Bon River; (c) rainfall (mm/hour) within the HEC-RAS simulation domain (observed during the 2020 event and simulated).

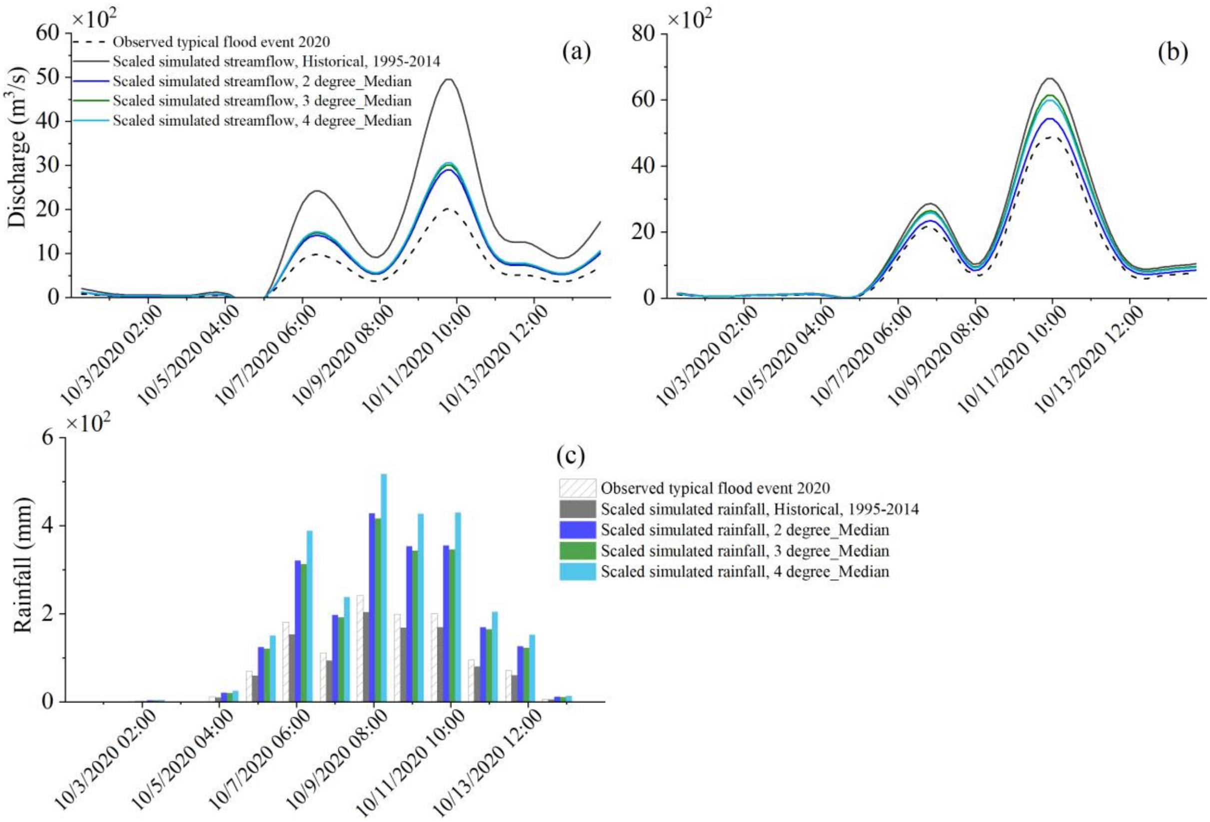

Table 5. The ratio of 5% AEP in simulated streamflow and simulated rainfall over the HEC-RAS simulation domain across the four scenarios (historical and 3 future GWLs) compared with the observed peak discharge of the 2020 flood event.

Ratio		Q at Thanh My	Q at Nong Son	Rainfall
Historical (5%)		2.47	1.37	0.85
2 Degrees (5%)	Lower	1.11	0.99	1.03
	Median	1.44	1.12	1.77
	Upper	1.94	1.54	2.30
3 Degrees (5%)	Lower	1.31	1.14	1.05
	Median	1.50	1.27	1.73
	Upper	1.83	1.58	2.31
4 Degrees (5%)	Lower	1.30	1.14	1.28
	Median	1.52	1.24	2.14
	Upper	1.78	1.91	2.92

3.4.3. Evaluation of the impact of the cascade dam and climate change on future flood inundation

By comparing scenarios at a GWL of 2°C, 3°C, and 4 °C against the historical reference period (1995–2014), which is assumed to reflect minimal reservoir influence, the results indicate that the cascading reservoir system is associated with a substantial reduction in flood extent and inundation depth across much of the downstream floodplain. The 2 and 3 °C scenarios show that many areas experiencing deeper inundation are shifted into the 0–0.5 m depth class, indicating that reservoir regulation primarily reduces flood depths (Figure 18). Under historical conditions, the flooded area exhibits an approximately linear decrease with higher inundation depth, whereas under reservoir regulation, the reduction becomes more pronounced for flood depths exceeding 0.5 m, except at 4°C of global warming. For flood depths exceeding 1 m, the inundated total area accounted for 60.0%, 67.7%, and 78.6% of the total inundated area under the 2, 3, and 4 °C GWL median scenarios, respectively. Compared to the historical period, these values represent relative changes of 0.71, 0.84, and 1.03, respectively. Notably, at 4°C GWL, intensified downstream rainfall substantially increased flood levels and diminished the regulating capacity of the reservoir. These findings suggest that future assessments should distinguish whether flooding is driven by upstream rainfall, downstream rainfall, or their combined effects. Furthermore, the results highlight that changes in inundation extent are both depth-dependent and spatially heterogeneous.

Considering both spatial distribution and total inundated area, flood extent exhibits a non-linear response to increasing warming levels. Under 2 °C GWL and 3 °C GWL median scenario, the simulated inundated areas (439.8 km^2 and 465.3 km^2, respectively) remain smaller than that of the historical reference period (481.8 km^2), suggesting that current reservoir regulation continues to exert a substantial flood-mitigation effect under certain warming conditions. However, under the stronger climate change scenario (GWL 4 °C), the inundated area increases to 490.0 km^2, exceeding both the historical baseline and the extent observed during the 2020 flood event (480 km^2). This transition indicates that the buffering capacity of reservoir operations may be progressively reduced as climate-driven increases in rainfall and runoff intensify. Model results suggest that upstream inflow contributes approximately 70% of the total discharge entering the hydraulic domain, while local rainfall over the floodplain accounts for about 30%. Because reservoir regulation primarily affects upstream inflows but cannot control rainfall-generated runoff within the lower basin, increased downstream rainfall under stronger warming conditions can partially offset or even exceed the mitigation effects of reservoir operations. These findings highlight that while reservoir systems may moderate flood impacts under moderate climate change, their capacity to compensate for intensified hydrological extremes may be limited under stronger warming scenarios.

Clear differences were also observed at the four downstream hydrological stations along the Vu Gia and Thu Bon Rivers. Compared with historical conditions, simulated values under all scenarios were lower, except for the 4 °C global warming scenario, which approached or exceeded the historical period (Figure 19). Notably, while the ranges between lower (25th percentiles) and upper (75th percentiles) estimates varied across scenarios, the distinctions were most consistently expressed in the median values. This supports the use of median estimates as a robust metric for detailed evaluation in this study, as they better capture the central tendency of the scenario responses while reducing the influence of extreme values.

Figure 18. (a–d) Spatial distribution of floodwater depth across the floodplain under the four scenarios. (e) Total flood inundation area by water-depth class for each scenario.

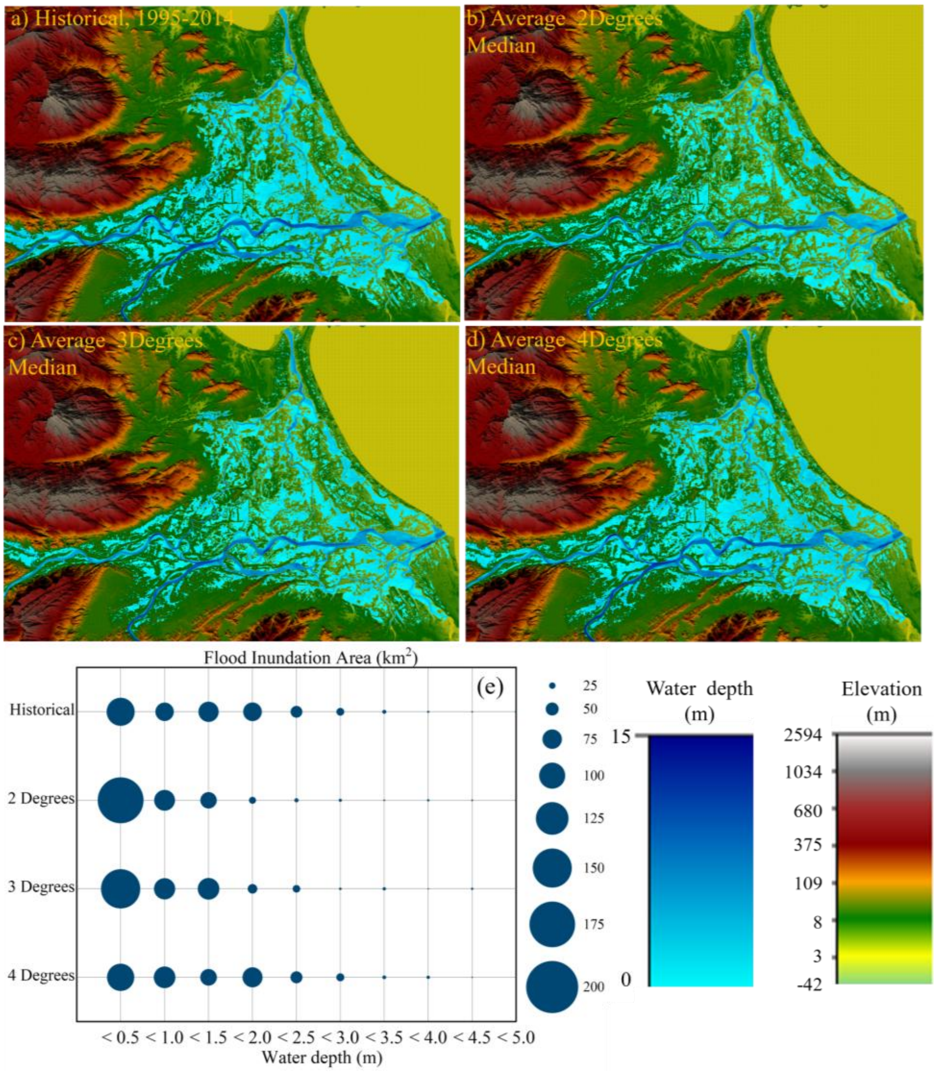

Figure 19. The hydrographs (water level in meter) at four representative hydrological stations for the historical period and GWLs 2°C, 3°C and 4°C. For each station and each GWL, the figure displays the hydrograph corresponding to the 25th, 50th and 75th percentile of 5% AEP streamflow.

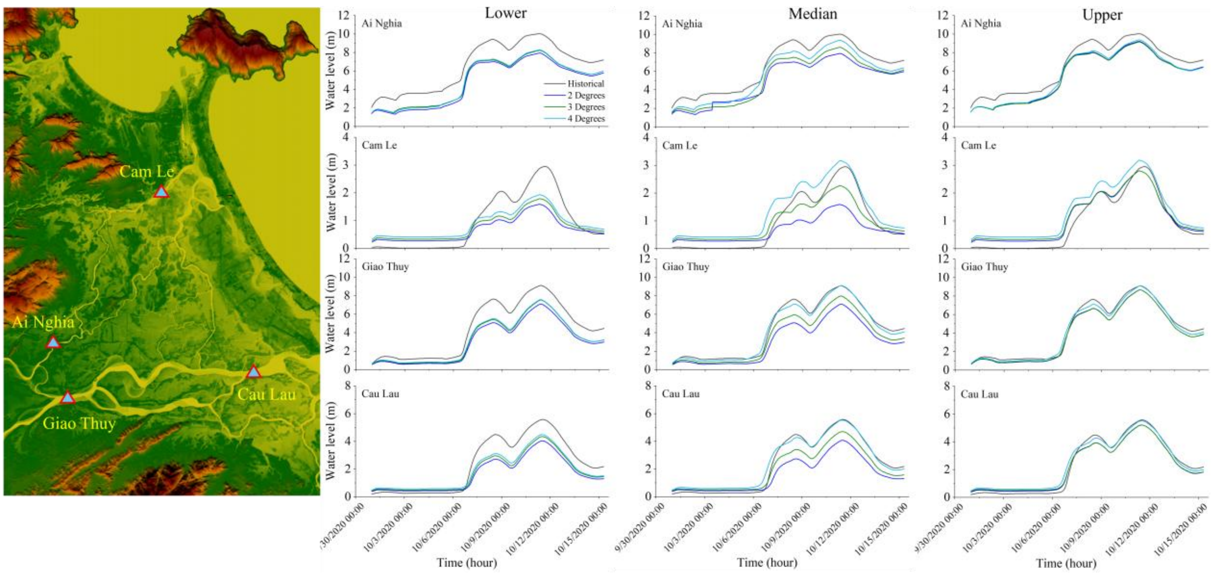

It should be noted that the present analysis does not explicitly isolate climate-change signals; nevertheless, the simulated patterns are consistent with broader evidence of climate-driven amplification of extreme precipitation (Figs. 13, 14, 15). Overall, the results suggest that cascading reservoirs can play an important role in reducing flood extent and depth, particularly for moderate inundation levels, while their ability to fully mitigate localized flooding under increasingly extreme climatic conditions may be constrained.

4. Discussion

This study illustrates the highly uncertain future of flood hazards over the downstream area of the Vu Gia – Thu Bon (VGTB) River, owing to the combined impacts of changes in climate forcing and existing water management strategies. The results also highlight the benefit of the cascade of dams and reservoirs across the mainstem, not only for hydropower generation but also for flood risk reduction. Specifically, the study highlights crucial roles of hydrological dams and the associated reservoirs in flood risk management, demonstrated through the substantially lower SOND as well as the 5% AEP streamflow simulated across the rest of the 21st century, regardless of which SSP is being considered. Despite these undisputed benefits, the complex climate characteristics of Central Vietnam together with the consistent intensification of extreme rainfall (the median values of 5% AEP rainfall projected by the 19 GCMs for the end of the century, regardless of SSP, show an increase of more than 20% relative to the magnitude simulated for the historical period) also indicate that it is extremely important to consider dam safety in a warming climate.

This careful assertation in future planning regarding dams is particularly more relevant in light of recent hydrologic disasters in Vietnam. In October 2025, the failure of Bac Khe 1 hydropower dam (in Lang Son, Northern Vietnam) was directly attributed to prolonged heavy rainfall, where the water inflow surged far beyond the spillway's design capacity (e.g., 1,572 m^3/s inflow versus 24 m^3/s designed flow). In the same month, a record-breaking flood also occurred in the Vu Gia Thu Bon River (since 1964), reaching a water level height of 5,52m, further highlighting that extreme rainfall can overwhelm both dam regulation capacity and downstream resilience. Recent investigations (Fischer et al., 2021) also suggest that "low-probability, high-impact" events are likely to appear more frequent in a warming climate, implying the urgent need new policies relevant to risks related to hazard magnitudes that are several standard deviations outside historical norms.

The large inter-model spread for rainfall projections remains one of the key challenges in developing new flood management policies. For instance, the 5% AEP of rainfall varies substantially across GCM-SSP combinations (Table 5), and the magnitude of the 50th and 75th percentile is much higher than the amount of historical 5% AEP (the scaling ratios identified under median and wet conditions range from 1.77 to 2.30 at a 2 °C GWL and from 1.73 to 2.31 at a 3 °C GWL, respectively). These uncertainties highlight another limitation of traditional approaches in flood design, which assumes that the observed frequency and magnitude of extreme events (e.g., the 5% AEP) will remain constant in the future. Nevertheless, climate change is altering the precipitation characteristics (Fowler et al., 2021), and the probability of an extreme storm is no longer “stationary”, making it possible for events that would have been classified as 100-year extreme rainfall events during the historical period (and subsequent hazardous flooding) to occur more often under a warmer climate.. Our assessment (see Figure 9b) also demonstrates this pattern: the 5% AEP rainfall tend to rise at a substantial rate over time, and the median values calculated in SSP2-4.5 and SSP5-8.5 reaches nearly 600 mm/day at the end of the century, much higher than the median intensity simulated over the historical period (well below 500mm/day). This finding, together with societal concern due to recent record-breaking rainfall over Central Vietnam (Bach Ma rain gauge recorded a staggering peak of 1,739 millimetres from 7 p.m. on 26/10/2025 to 7 p.m. on 27/10/2025, the highest ever recorded in Vietnam and the second-largest record globally) suggests the need to explore a new approach in dealing with flood hazards in a highly uncertain future.

Estimation of annual exceedance probabilities (AEPs) is subject to substantial uncertainty due to limited sample sizes, distributional assumptions, and potential non-stationarity. While the 48-year historical record supports estimation of the 5% AEP using the annual maxima series (AMS)/block-maxima (BM) method and GEV fitting, sampling variability remains significant. Uncertainty is amplified in future periods based on a shorter period of 20-year windows, leading to poorly constrained tail behavior and wide confidence intervals, with results sensitive to individual events and to the choice between AMS/BM and peak over threshold (POT) methods. Moreover, the assumption of stationarity may be violated under climate change and dams, complicating the interpretation of projected flood quantiles. More extreme events (i.e., 1% AEP floods) were not examined here but are expected to exhibit even larger uncertainty and stronger sensitivity to changes in precipitation extremes, warranting future investigation.

Streamflow simulations were generated using an ensemble of climate models across three SSPs and three global warming levels (GWLs). To represent climate model uncertainty, the 25th, 50th, and 75th percentiles of the simulated streamflow ensemble were calculated, corresponding to dry, median, and wet streamflow scenarios, respectively. This study accounts for climate model uncertainty by employing a multi-model ensemble across multiple SSPs and global warming levels, with streamflow responses summarized using percentile-based scenarios. While this approach captures a substantial portion of inter-model variability, it does not fully represent uncertainties related to internal climate variability, model structural differences, or extremes beyond the sampled ensemble. Future research should expand the analysis to all GCMs to investigate the consistency across all models in projecting flood risks under different warming levels and emission pathways. It is also important to investigate the risks related to higher flood magnitude (e.g., 1% AEP), as more "record-shattering" events have been observed recently. Furthermore, integrating non-stationary frequency analysis and process-based evaluation of climate models would improve the robustness of projected hydrological impacts.

It is important to note that this study has not fully examined potential changes in flood dynamics under new infrastructure development, such as the North-South high-speed railway connecting Hanoi and Ho Chi Minh City, which was approved for construction to start by 2027 and completion by 2035. To provide a holistic assessment of such modelling practice, there is an urgent need for regional cooperation in data sharing and the adoption of high-resolution LiDAR-derived topographic data, which is crucial for increasing the accuracy of future flood risk assessments. Specifically, establishing a central hub for hydroclimatic (e.g., observed rainfall, river discharge, river water level…) and geographic data (e.g., land use types, soil types, topography…), inter-reservoir operating data (timeseries variables, inter-reservoir linkage variables, operating rules, system-level attributes,…) – which are currently coordinated by different agencies within the Ministry of Agriculture and Environment (e.g., Vietnam Disaster and Dyke Management Authority, Vietnam Hydro-Meteorological Administration, Institute of Water Resources Planning, Vietnam Academy of Water Resources, Department Of Survey, Mapping and Geographic Information Viet…) – will shape better data-informed decisions by the public and policymakers in water management and flood control.

5. Conclusions

This study utilized a coupled SWAT-HEC-RAS modelling framework to assess the future flood inundation in the Vu Gia Thu Bon River Basin, providing a critical insight into how climate change and current dam operation policies modulate flood risk in Central Vietnam. Using multiple climate change scenarios and GCMs, the study has thoroughly assessed flood inundation extent and depth in the VGTB Basin, demonstrating a substantial exacerbation of flood risk across the high-exposure downstream areas in the most extreme scenario (the wet condition corresponding to a 4°C global warming level).

While upstream reservoir operations have the potential to cut off peak water levels and reduce flooded areas by providing essential storage during extreme events, they also introduce significant complexities into the flood propagation dynamics of the VGTB Basin. Based on these findings, it is recommended that policy frameworks transition toward an integrated water resource management approach that explicitly links climate projections with reservoir management protocols to ensure the balance between economic benefits and public safety. A potential approach is to use the bottom-up approach to explore the maximum operational adaptive capacity of the recent dam cascade under the space of possible future hydrometeorological states. To achieve this objective, it is important to accurately understand all stakeholders' demands to identify system failure criteria and carefully revisit the constraints of the current policy underlying dam operation. In addition, policymakers should implement stricter land-use regulations to prevent the exposure of new infrastructure in areas identified as highly susceptible to future flood hazards. The adaptation of these multi-dimensional policies will ensure that flood mitigation strategies are resilient to the highly uncertain states of future flood hazards and provide a robust foundation for long-term balance in social and economic security in Central Viet

Bibliography

ADRC (2000). Viet Nam: Flood – 1999/11.

APN (2021). Integrated Flood and Sediment MAnagement in River basins for susTainable development (FSMART). DOI:https:// doi.org/10.30852/p.13 492

Callaghan, D.P. and Hughes, M.G. (2022). Assessing flood hazard changes using climate model forcing. *Nat. Hazards Earth Syst. Sci.*, 22(8): 2459-2472. DOI:10.5194/nhess-22-2459-2022

Diop, S. B., Ekolu, J., Tramblay, Y., Dieppois, B., Grimaldi, S., Bodian, A., Blanchet, J., Rameshwaran, P., Salamon, P. and Sultan, B. (2025). Climate change impacts on floods in West Africa: new insight from two large-scale hydrological models. *Nat. Hazards Earth Syst. Sci.*, 25(9): 3161-3184. DOI:10.5194/nhess-25-3161-2025

Douville, H., K. Raghavan, J. Renwick, R.P. Allan, P.A. Arias, M. Barlow, R. Cerezo-Mota, A. Cherchi, T.Y. Gan, J. Gergis, D. Jiang, A. Khan, W. Pokam Mba, D. Rosenfeld, J. Tierney, and O. Zolina (2021). Water Cycle Changes. In: Intergovernmental Panel on Climate, C. (Ed.), Climate Change 2021 – The Physical Science Basis: Working Group I Contribution to the Sixth Assessment Report of the Intergovernmental Panel on Climate Change. Cambridge University Press, Cambridge, pp. 1055-1210. DOI: 10.1017/9781009157896.010

Dysarz, T., Marcinkowski, P., Wicher-Dysarz, J., Piniewski, M., Mirosław-Świątek, D. and Kundzewicz, Z. W. (2025). Assessment of Climate Change Impact on Flood Hazard Zones. *Water Resources Management*, 39(2): 963-977. DOI:10.1007/s11269-024-04002-8

Fischer, E. M., Sippel, S. and Knutti, R. (2021). Increasing probability of record-shattering climate extremes. *Nature Climate Change*, 11, 689–695. https:// doi.org/10.1038/s41558-021-01092-9

Fowler, H.J., Lenderink, G., Prein, A.F., Westra, S., Allan, R.P., Ban, N., Barbero, R., Berg, P., Blenkinsop, S., Do, H.X. and Guerreiro, S. (2021). Anthropogenic intensification of short-duration rainfall extremes. *Nature Reviews Earth & Environment*, 2(2), pp.107-122.

Gassman, P.W., Reyes, M.R., Green, C.H. and Arnold, J.G. (2007). The soil and water assessment tool: historical development, applications, and future research directions. *Transactions of the ASABE*, 50(4), pp.1211-1250.

Gyuleva, G., Fischer, E., Knutti, R., & Sippel, S. (2026). Recent Temperature and Energy Imbalance Trends Point to Higher Estimates of Future Warming. *Earth's Future, 14*(8), e2026EF008356, doi:10.1029/2026EF008356

Hausfather, Z., Marvel, K., Schmidt, G.A., Nielsen-Gammon, J.W. and Zelinka, M. (2022). Climate simulations: recognize the "hot model" problem. *Nature* 605(7908), pp.26-29.

Ilyas, A. M., Pham, Q. B., Zhu, D., Elahi, E., Linh, N. T. T., Anh, D. T., Khedher, K. M. and Ahmadlou, M. (2021). Multi sources hydrological assessment over Vu Gia Thu Bon Basin, Vietnam. *Hydrological Sciences Journal*, 66(8): 1383-1392. DOI:10.1080/02626667.2021.19359 64

IPCC (2021). Climate Change 2021: The Physical Science Basis. Contribution of Working Group I to the Sixth Assessment Report of the Intergovernmental Panel on Climate Change [Masson-Delmotte, V., P. Zhai, A. Pirani, S.L. Connors, C. Péan, S. Berger, N. Caud, Y. Chen, L. Goldfarb, M.I. Gomis, M. Huang, K. Leitzell, E. Lonnoy, J.B.R. Matthews, T.K. Maycock, T. Waterfield, O. Yelekçi, R. Yu, and B. Zhou (eds.)]. Cambridge University Press, Cambridge, United Kingdom and New York, NY, USA, 2391 pp.

IPCC (2023). Climate Change 2022 – Impacts, Adaptation and Vulnerability: Working Group II

Contribution to the Sixth Assessment Report of the Intergovernmental Panel on Climate Change. Cambridge University Press, Cambridge. DOI: 10.1017/9781009325844

IFRC (2022). Vietnam: Floods – Final Report, Operation n° MDRVN020.

Kundzewicz, Z. W., Su, B., Wang, Y., Wang, G., Wang, G., Huang, J. and Jiang, T. (2019). Flood risk in a range of spatial perspectives – from global to local scales. *Natural Hazards and Earth System Sciences*, 19(7): 1319-1328. DOI:10.5194/nhess-19-1319-2019

Lima, F.N., Freitas, A.C. and Silva, J. (2023). Climate Change Flood Risk Analysis: Application of Dynamical Downscaling and Hydrological Modelling, *Atmosphere*, *14*(7), 1069. DOI:10.3390/atmos14071069

Luo, P., Mu, D., Xue, H., Ngo-Duc, T., Dang-Dinh, K., Takara, K., Nover, D. and Schladow, G. (2018). Flood inundation assessment for the Hanoi Central Area, Vietnam under historical and extreme rainfall conditions. *Scientific Reports*, 8(1): 12623. DOI:10.1038/s41598-018-30024-5

Merz, B., Blöschl, G., Vorogushyn, S., Dottori, F., Aerts, J. C., Bates, P., Bertola, M., Kemter, M., Kreibich, H., Lall, U. and Macdonald, E. (2021). Causes, impacts and patterns of disastrous river floods. *Nature Reviews Earth & Environment*, 2(9): 592-609. DOI:10.1038/s43017-021-00195-3

MoNRE (2016). National topographic map at a scale of 1:10,000.

MoNRE (2020). Climate change scenarios in Vietnam.

Mudashiru, R.B., Sabtu, N., Abustan, I. and Balogun, W. (2021). Flood hazard mapping methods: A review. *Journal of Hydrology*, 603: 126846. DOI:https:// doi.org/10.1016/j.jhydrol.2021.126846

Nguyen, M. T., Sebesvari, Z., Souvignet, M., Bachofer, F., Braun, A., Garschagen, M., Schinkel, U., Yang, L. E., Nguyen, L. H. K., Hochshield, V., Assmann, A. and Hagenlocher, M. (2021). Understanding and assessing flood risk in Vietnam: Current status, persisting gaps, and future directions. *Journal of Flood Risk Management*, 14(2): e12689. DOI:https:// doi.org/10.1111/jfr3.12689

Nguyen, B. Q., Kantoush, S., Binh, D. Van, Saber, M., Vo, D. N. and Sumi, T. (2023a). Quantifying the impacts of hydraulic infrastructure on tropical streamflows. *Hydrological Processes*, 37(3). https:// doi.org/https:// doi.org/10.1002/hyp.14834

Nguyen, B. Q., Kantoush, S., Binh, D. Van, Saber, M., Vo, D. N. and Sumi, T. (2023b). Understanding the anthropogenic development impacts on long-term flow regimes in a tropical river basin, Central Vietnam. *Hydrological Sciences Journal*, 1–14.

Nguyen, H. D., Dang, D. K., Hoang, T. S., Truong, Q. H., Nguyen, T. N. U., Nguyen, X. L. and Ha, M. C. (2024). Flood hazard assessment using machine learning and hydrodynamic modelling: case study in the Vu Ga–Thu Bon basin in Vietnam. *Water Practice and Technology*, 19(10): 4104-4127. DOI:10.2166/wpt.2024.242

Nguyen, B. Q., Kantoush, S. A., Dinh, Q. N., Nguyen, V. T. and Sumi, T. (2024a). Investigation of the main drivers influencing sediment property change and coastal erosion in Central Vietnam. *Interpretation*, 13(3), 1–37.

Nguyen, B. Q., Kantoush, S. A. and Sumi, T. (2024b). Quantifying the consequences of unsustainable sand mining and cascade dams on aspects in a tropical river basin. *Scientific Reports*, 14(1), 1178. https:// doi.org/10.1038/s41598-024-51405-z

Nguyen, B. Q., Kantoush, S. A., Van Binh, D. and Sumi, T. (2024c). An assessment of uncontrolled human interventions on the contemporary sediment budget and morphological alterations of the Vu Gia Thu Bon River basin, central Vietnam. Heliyon.

Nguyen, B. Q., Kantoush, S. A., Vo, N. D. and Sumi, T. (2024d). Framework for reservoir sedimentation estimation using the hydrological model and campaign—A case study of A Vuong Reservoir in central Vietnam. *International Journal of Sediment Research*, *40*(1), 78-90.

Nguyen, B. Q., Kantoush, S. A., Nguyen, T. H., Bui, T. T. P., Nguyen, P. S., Doan, T. N. C. and Vo, D. N. (2025a). Cumulative impacts of interbasin water transfer and salinity intrusion on water security in central Vietnam. *Science of The Total Environment*, 998, 180250.

Nguyen, B. Q., Kantoush, S. A., Nguyen, T. H., Sumi, T. and Kobayashi, S. (2025b). Long-term assessment of hydropeaking and cumulative impacts on sediment transport, grain size dynamics, channel stability and water resource management. *Journal of Environmental Management*, 380, 124983.

Nguyen, B. Q., Kantoush, S. A. and Sumi, T. (2025c). Assessing the multidimensional impacts of riverbed sand mining on geomorphological change and water transfer rate: A comprehensive investigation of Central Vietnam's Vu Gia Thu Bon River system. *Journal of Hydrology*, 132853.

Nguyen, B. Q., Kantoush, S. A., Tran, T. and Sumi, T. (2025d). Human-Induced Hydrological Droughts in Central Vietnam: A Study for River-Segment Analysis. *Hydrological Processes*, 39(7), e70206.

Nguyen-Duy, T., Ngo-Duc, T. and Desmet, Q. (2023). Performance evaluation and ranking of CMIP6 global climate models over Vietnam. *Journal of Water and Climate Change*, 14(6), pp.1831-1846.

Pham, N. H., Takara, K. and Son, N. H. (2015). Flood Hazard Impact Analysis in the Downstream of Vu Gia-Thu Bon River System, Quang Nam Province, Central Vietnam. *Journal of Japan Society of Civil Engineers, Ser. B1 (Hydraulic Engineering)*, 71(4): I_157-I_162. DOI:10.2208/jscejhe.71.I_157

Pham, H.T., Marshall, L., and Johnson, F. (2021). Daily time series of river water levels derived from a seasonal linear model using multisource satellite products under uncertainty. *Journal of Hydrology*, 602: 126783. DOI:https:// doi.org/10.1016/j.jhydrol.2021.126783

Pham, H.T., Marshall, L., Johnson, F. and Sharma, A. (2018). A method for combining SRTM DEM and ASTER GDEM2 to improve topography estimation in regions without reference data. *Remote Sensing of Environment*, 210: 229-241.

Phuong, D. N. D., Duong, T. Q., Liem, N. D., Tram, V. N. Q., Cuong, D. K. and Loi, N. K. (2020). Projections of Future Climate Change in the Vu Gia Thu Bon River Basin, Vietnam by Using Statistical DownScaling Model (SDSM). *Water*, *12*(3), 755 . DOI:10.3390/w12030755

Riahi, K., van Vuuren, D. P., Kriegler, E., Edmonds, J., O'Neill, B. C., Fujimori, S., Bauer, N., Calvin, K., Dellink, R., Fricko, O., Lutz, W., Popp, A., Cuaresma, J. C., Kc, S., Leimbach, M., Jiang, L., Kram, T., Rao, S., Emmerling, J., ... Tavoni, M. (2017). The Shared Socioeconomic Pathways and their energy, land use, and greenhouse gas emissions implications: An overview. *Global Environmental Change*, 42, 153–168.

Savino, M., Todaro, V., Maranzoni, A. and D'Oria, M. (2023). Combining Hydrological Modelling and Regional Climate Projections to Assess the Climate Change Impact on the Water Resources of Dam Reservoirs. *Water*. *15*(24), 4243. DOI:10.3390/w15244243

SCS (1972). National Engineering Handbook, Section 4: Hydrology. Department of Agriculture, Washington DC.

Seneviratne, S.I., X. Zhang, M. Adnan, W. Badi, C. Dereczynski, A. Di Luca, S. Ghosh, I. Iskandar, J. Kossin, S. Lewis, F. Otto, I. Pinto, M. Satoh, S.M. Vicente-Serrano, M. Wehner, and B. Zhou (2021). Weather and Climate Extreme Events in a Changing Climate. In: Intergovernmental Panel on Climate, C. (Ed.), Climate Change 2021 – The Physical Science Basis: Working Group I Contribution to the Sixth Assessment Report of the Intergovernmental Panel on Climate Change. Cambridge

University Press, Cambridge, pp. 1513-1766. DOI: 10.1017/9781009157896.013

Sharma, S., Gomez, M., Keller, K., Nicholas, R.E., and Mejia, A. (2021). Regional Flood Risk Projections under Climate Change. *Journal of Hydrometeorology*, 22(9): 2259-2274. DOI:https://doi.org/10.1175/JHM-D-20-0238.1

Slangen, A.B., Palmer, M.D., Camargo, C.M., Church, J.A., Edwards, T.L., Hermans, T.H., Hewitt, H.T., Garner, G.G., Gregory, J.M., Kopp, R.E. and Santos, V.M. (2023). The evolution of 21st century sea-level projections from IPCC AR5 to AR6 and beyond. Cambridge Prisms: Coastal Futures, 1, p.e7.

Tabari, H. (2020). Climate change impact on flood and extreme precipitation increases with water availability. *Scientific Reports*, 10(1): 13768. DOI:10.1038/s41598-020-70816-2

To, T.N., Vu, H.C. and Le, H. (2022). Impacts of reservoir operation and urbanization on flood inundation in the Vu Gia Thu Bon Basin, Vietnam. *Water Supply*, 22(4): 4656-4675. DOI:10.2166/ws.2022.124

Tran-Anh, Q., Ngo-Duc, T., Espagne, E. and Trinh-Tuan, L. (2023). A 10-km CMIP6 downscaled dataset of temperature and precipitation for historical and future Vietnam climate. *Scientific Data*, 10(1), p.257.

USACE (2024). 2D Modelling User's Manual, Version 6.6 (2021).

van Vuuren, D. P., O'Neill, B. C., Tebaldi, C., Sanderson, B. M., et al. (2026). the scenario model intercomparison project for cmip7 (scenariomip-cmip7). *Geoscientific Model Development*, 19: 2627–2656. DOI:https://doi.org/10.5194/gmd-19-2627-2026

Vo, N.D. and Gourbesville, P. (2016). Model Uncertainty in Flood Modelling. Case Study at Vu Gia Thu Bon Catchment - Vietnam. *Procedia Engineering*, 154: 450-458. DOI:https://doi.org/10.1016/j.proeng.2016.07.537

Vu, M.T., Vo, N.D., Gourbesville, P., Raghavan, S.V. and Liong, S.Y. (2017). Hydro-meteorological drought assessment under climate change impact over the Vu Gia–Thu Bon river basin, Vietnam. *Hydrological Sciences Journal*, 62(10): 1654-1668. DOI:10.1080/02626667.2017.1346374

Wang, S., Ancell, B., Yang, Z.-L., Duan, Q. and Anagnostou, E.N. (2022). Hydroclimatic extremes and impacts in a changing environment: Observations, mechanisms, and projections. *Journal of Hydrology*, 608: 127615. DOI:https://doi.org/10.1016/j.jhydrol.2022.127615.

List of acronyms and abbrevations

ADRC	Asian Disaster Reduction Center
AEP	Annual Exceedance Probability
AFD	Agence Française de Développement
ALOS	Advanced Land Observing Satellite
AMAX	Annual maxima
AMS	Annual maxima series
AR5	IPCC's Fifth Assessment Report
AR6	IPCC's Sixth Assessment Report
ASTER	Advanced Spaceborne Thermal Emission and Reflection Radiometer
BM	Block Maxima
CMIP5	Coupled Model Intercomparison Project Phase 5
CMIP6	Coupled Model Intercomparison Project Phase 6
CMIP6-VN	Downscaled CMIP6 dataset for Viet Nam
CN	Curve Number
DEM	Digital Elevation Model
DPSIR	Driver-Pressure-State-Impact-Response
DWE	Diffusion Wave Equations
GCM	Global Climate Model
GDEM2	Global Digital Elevation Model Version 2
GDP	Gross Domestic Product
GEV	Generalised Extreme Value
GHG	Greenhouse Gas
GIS	Geographic Information System
GWL	Global Warming Level
HEC-RAS	Hydrologic Engineering Center's River Analysis System
HRU	Hydrologic Response Unit
ICEM	International Centre for Environmental Management
IFRC	International Federation of Red Cross and Red Crescent Societies
IPCC	Intergovernmental Panel on Climate Change
JAXA	Japan Aerospace Exploration Agency
JEL	Journal of Economic Literature
KGE	Kling-Gupta Efficiency
LiDAR	Light Detection and Ranging
LULC	Land Use and Land Cover
MoNRE	Ministry of Natural Resources and Environment
NOAA	National Oceanic and Atmospheric Administration
NSE	Nash-Sutcliffe Efficiency
PBIAS	Percent Bias
POT	Peak Over Threshold

R	**Pearson correlation coefficient**
RCP	**Representative Concentration Pathway**
RMSE	**Root Mean Squared Error**
RSR	**RMSE-standard deviation ratio**
Rx1day	**Annual maximum 1-day rainfall**
SCS	**Soil Conservation Service**
SCS-CN	**Soil Conservation Service Curve Number**
SDSM	**Statistical DownScaling Model**
SLR	**Sea-Level Rise**
SOND	**September-October-November-December**
SRTM	**Shuttle Radar Topography Mission**
SSP	**Shared Socioeconomic Pathway**
SWAT	**Soil and Water Assessment Tool**
SWE	**Shallow Water Equations**
TCVN	**Tieu Chuan Viet Nam / Vietnamese National Standard**
USACE	**U.S. Army Corps of Engineers**
USD	**United States Dollar**
VGTB	**Vu Gia Thu Bon**
VND	**Vietnamese dong**

Appendix

Appendix 1 - Characteristics of annual flow

The Vu Gia Thu Bon basin has high rainfall and intensity, and the river has almost no middle section, so the flood rushes downstream quite suddenly, the flood amplitude, flood intensity and flood level are quite high, often causing serious flooding in the downstream area. The dry season lasts from January to October (9 months), with the total average flow volume in the dry season accounting for about 35.2% of annual total flows W_{year}. The total average flow volume of the three smallest months from March to May accounts for about 8.45% of W_{year}. The smallest discharge per unit area M_{min} varies from 4 – 6 l/s.km^2. Figure A.1 highlights the strong seasonal cycle of the streamflow of the Vu Gia – Thu Bon river basin. The figure also demonstrates the high year-to-year variation of flood flows, further, confirming the pressing demands of improving disaster management policies in the region in a changing climate.

Figure A.1 Boxplots of monthly average values of daily streamflow (1980–2023) recorded at Thanh My (left) and Nong Son (right) river streamflow gauges.

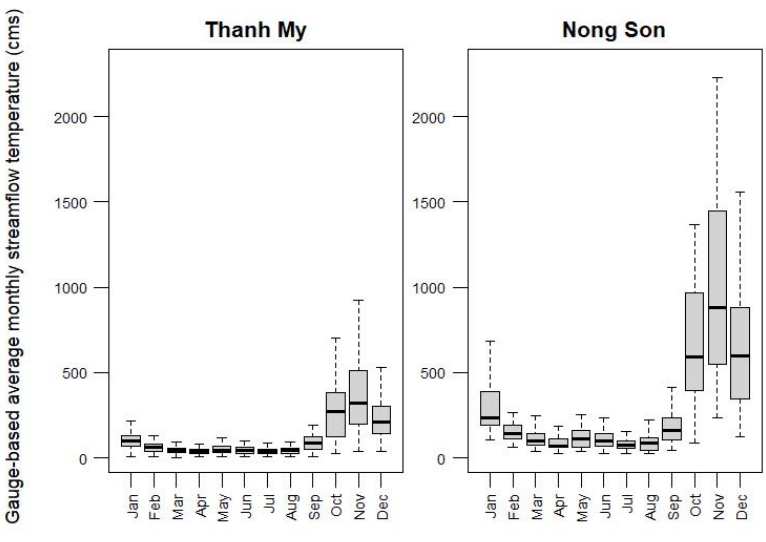

- ***On Vu Gia River***

According to monitoring data from 1980–2023 at Thanh My hydrological station, the basin area is F = 1,850 km^2, the long-term mean annual flow is Qo = 118 m^3/s, corresponding to the long-term mean annual discharge per unit area Mo = 63.0 l/s/km^2, the long-term total average annual surface flow Wo = 3.91 km^3 ; flood season from October to December, the total average surface flow volume of flood season is W $_{TB}$ flood season = 2.39 km^3, accounting for about 61.1% W_{year}, the largest average monthly flow volume is September, accounting for about 25.1% Wyear, the largest observed flow volume is Q_{max} = 7,000 m^3/s (20/11/1998) corresponding to the largest discharge per unit area of M_{max} = 3,784 $l/s/km^2$; and the dry season lasts from January to October (9 months), with the average total flow of the dry season being about 38.9% of W_{year} , the average total flow of the three smallest months is about 9.65% of W year, the average flow of the smallest month is about 2.80% of W_{year}, the smallest flow Q_{min} = 11.3 m^3/s (July 27, 1988), corresponding to the smallest discharge per unit area M_{min} = 6.11 $l/s/km^2$.

- ***On Thu Bon River***

According to monitoring data from 1980–2023 at Nong Son hydrological station: long-term mean annual flow is Qo = 306 m^3/s, corresponding to long-term mean annual discharge per unit area Mo = 97.0 $l/s/km^2$, long-term total average annual surface flow Wo = 8 .61 km^3; Flood season from October to December, the total average surface flow of the flood season is W_{TB} flood season = 5.84 km^3, accounting for about 67.8% W_{year}, the average flow of the largest month (November) accounts for about 29.0% W_{year}, the largest observed flow is Q_{max} = 10,815 m^3/s (12/11/2007), corresponding to the largest discharge per unit area Mmax = 3,433 $l/s/km^2$, the dry season lasts from January to October (9 months), the total average flow of the dry season (W_{TB} dry season) accounts for about 32.2% W_{year}, the total average flow of the three smallest months (VI-VIII) accounts for about 7.57% W year, the average flow of the smallest month (VII) accounts for about 2.15% W_{year}, the smallest flow is Q_{min} = 14.6 m^3/s (21/8/1977), corresponding to the smallest discharge per unit area M_{min} = 4 .63 $l/s/km^2$.

- ***Annual flow variances***

According to actual measurements at Nong Son and Thanh My stations, the variance of the annual flow of the Vu Gia and Thu Bon rivers is not very large. The coefficient of variance of the annual flow on the Thu Bon River is 0.61, while on the Vu Gia River, the annual flow coefficient of variance of 0.60. Table A1 shows annual flow statistics at the stations in the study area.

Table A.1. Key statistics of streamflow regimes (1980–2023) at two stations in the basin.

Station	Long-term mean annual flow Q_o	Coefficient of variance C_v	Coefficient of skewness C_s	Designed flood with AEP $Q_{p(\%)}$ (m^3/s)						Catchment area F_{lv} (km^2)
				10	25	50	75	85	90	
Thanh My	118	0.60	7.45	185	143	113	92.8	73.1	59.6	1,850
Nong Son	306	0.61	6.26	426.2	368.9	277.8	236.8	225.0	203.1	3,150

Appendix 2 - Flood characteristics in the Vu Gia Thu Bon River basin

The flow regime on rivers in Quang Nam province depends entirely on the flow regime on the Vu Gia Thu Bon River basin. According to the assessment of the officers of the Flood and Storm Prevention Command of Quang Nam province, the flow at Cau Lau station has a direct correlation with the flood and inundation situation of the whole province. With a short flood season, floods often occur consecutively in a short period, creating a flood process curve with many peaks.

The flood season only occurs in 3 months from October to December, but the flow volume accounts for 60 – 70% of the annual flow volume. In Quang Nam, on average, there are 4 floods from level I or higher each year, with the highest number of 8 to 9 floods per year, resulting in the phenomenon of "flood after flood" or "flood on flood" as happened in 2007. October and November are the two months when large floods often occur, with particularly large floods in 1998, 1999, 2007, 2009, 2013, 2017, 2018, and 2020.

Floods and inundation are the most damaging natural disasters to people, property, and infrastructure across the province. From 1997 to 2016, floods caused 668 deaths and 1,656 injuries. Damage to property and infrastructure reached VND 12,232.95 billion. Through statistics on flood damage, we can see that human and economic losses from major floods occur at a rate quite similar to the magnitude of the flood. Some major floods in recent years have shown this, such as the big Floods in 2020 (Figure A.2). During the 2020 rainy season, Hoi An ancient town suffered a total of 7 floods. Notably, from the beginning of November until now, people living in the ancient town have experienced 2 floods, and many streets in Hoi An ancient town were deeply submerged in water. On the morning of November 30, floods from upstream and heavy rain caused some streets along the Hoai River, Hoi An City to be surrounded by floodwaters. At nearly 9:00 a.m., Bach Dang, Nguyen Phuc Chu, and Cong Nu Ngoc Hoa streets were flooded 20 to 50 cm, with muddy water reaching the doors of houses and shops.

Figure A.2. Images of the 2020 big flood.

Source : https:// dantri.com.vn/xa-hoi/pho-co-hoi-an-ngap-lut-lan-thu-5-trong-vong-1-thang-20201107115334884.htm

Appendix 3 - Supplementary data

Figure A.3 Boxplots of monthly rainfall over the 1980–2023 period across 16 rain-gauges over the Vu Gia Thu Bon River basin.

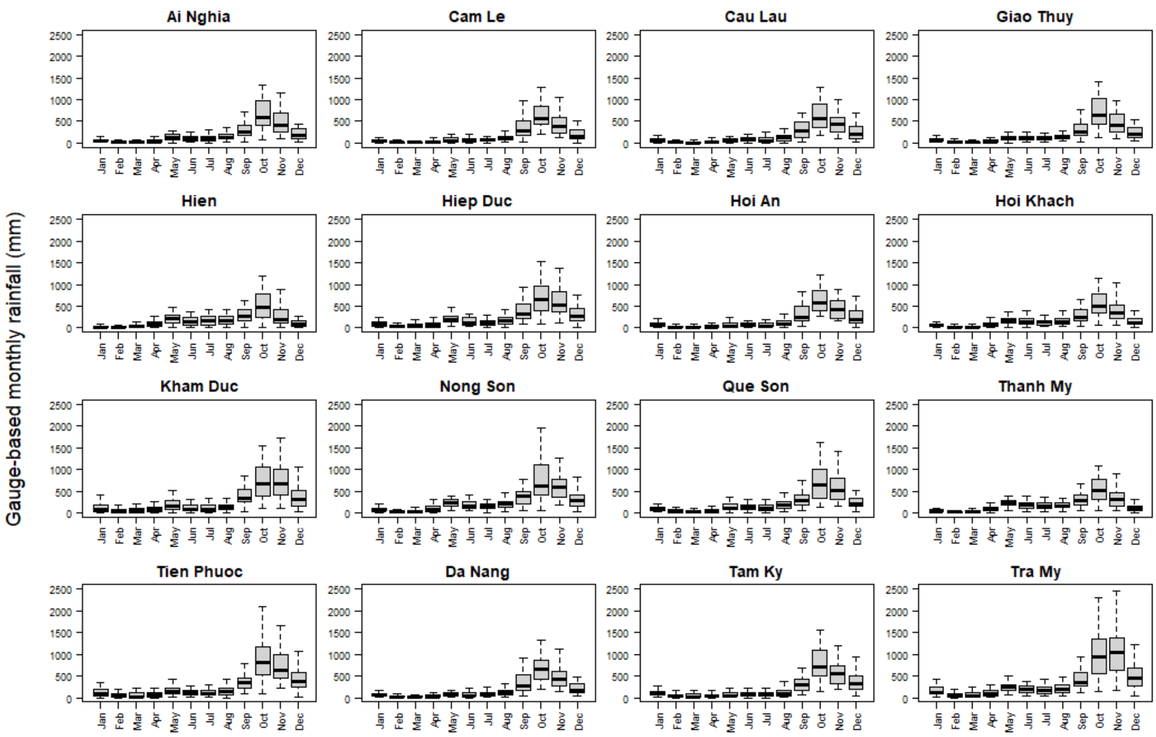

Figure A.4. Variabilities of hydro-climatic factors over the Vu Gia Thu Bon River basin at the monthly time step. The dark black line represents the moving 3-month average for each variable. The Oceanic Niño Index was obtained from NOAA.

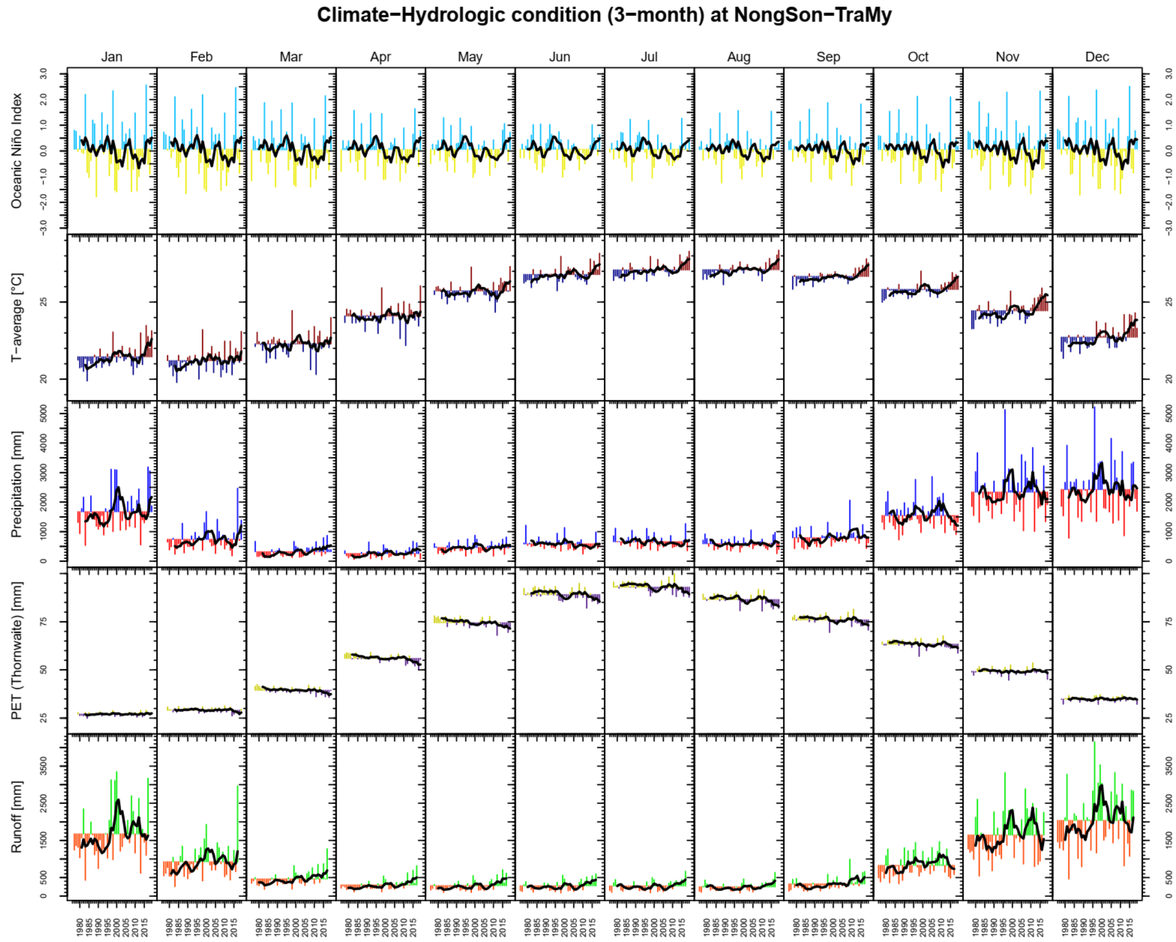

Source: https:// origin.cpc.ncep.noaa.gov/

Table A2. Profile of 18 reservoirs across the VGTB River basin.

Name	Catchment area	Dead water level (DWL)	Normal water level (NWL)	Flood design water level (FWL)	Total storage	Active storage	Dead storage	Turbine discharge	First year of operation
Unit	km^2	m	m	m	$10^6 m^3$	$10^6 m^3$	$10^6 m^3$	m^3/s	Year
A Vuong	682	340	380	382.2	343.55	266.48	77.07	78.4	2008
A Vuong 3	258.4	551.6	552.5	559.45	2.94	0.44	2.5	22.7	2016
Song Tranh 2	1100	140	175	178.51	729.2	521.1	208.1	245	2011
Song Tranh 3	1450	70.5	71.5	75.9	34.1	3.1	31	301.6	2013
Song Tranh 4	1610	45.5	46.5	-	24.81	3.32	21.49	298	2020
Dak Mi 2	445	624	630	635.19	1.611	0.692	0.919	44.36	2019
Dak Mi 3	612	353	359	363.96	5	2.304	2.696	76	2017
Dak Mi 4	1125	240	258	260.33	312.38	158.26	154.12	128	2011
Dak Mi 4B	29	105	105.3	107.28	0.688	0.066	0.622	130	2012
Dak Mi 4C	82.6	66.2	67.2	68.86	2.67	0.52	2.15	140	2012
Song Bung 4	1448	205	222.5	228.11	510.8	233.99	276.81	166	2015
Song Bung 4A	2276	95.4	97.4	99.95	10.6	1.58	9.02	166.4	2012
Song Bung 5	2369	58.5	60	64	20.27	2.45	17.82	239.24	2013
Song Bung 6	2386	31.8	31.8	45.89	3.29	0	3.29	239.8	2012
Za Hung	537	445	450	457.27	1.12	0.74	0.38	53.4	2009
Khe Dien	72	187.4	206.94	211.78	50.98	50.35	0.63	11.3	2007
Song Con 2	81	319	340	345.68	29.19	25.41	3.78	9.7	2009
An Diem 2	169.8	344	348.5	353.34	0.28	0.19	0.09	9	2010

Table A3. Meteorological and hydrological station name, location and monitoring period of the rainfall observation data.

Seq	Station name	Location		Time monitoring	Variables
		Longitude	Latitude		
1.	Ai Nghia	15.8739996	108.1039963	1978 - 2023	X, H
2.	Cam Le	16.01300049	108.2060013	1978 - 2023	X, H
3.	Cau Lau	15.85999966	108.2789993	1978 - 2023	X, H
4.	Da Nang	16.04500008	108.2070007	1978 - 2023	X, T
5.	Giao Thuy	15.83899975	108.1269989	1978 - 2023	X, H
6.	Hien	15.91699982	107.6460037	1978 - 2023	X
7.	Hiep Duc	15.57800007	108.1019974	1978 - 2023	X
8.	Hoi An	15.86999989	108.3649979	1978 - 2023	X, H
9.	Hoi Khach	15.82699966	107.9189987	1978 - 2023	X, H
10.	Kham Duc	15.42700005	107.7900009	1978 - 2023	X
11.	Nong Son	15.69999981	108.0329971	1978 - 2023	X, H, Q
12.	Que Son	15.69999981	108.0999985	1978 - 2023	X
13.	Thanh My	15.7670002	107.8330002	1978 - 2023	X, H, Q
14.	Tien Phuoc	15.4829998	108.3000031	1978 - 2023	X
15.	Tra My	15.35000038	108.2330017	1978 - 2023	X, T
16.	Tam Kỳ	15.553631	108.497419	1978 - 2023	X, T

Note : X is rainfall, T is temperature, H is water level and Q is discharge.

Figure A5. Locations of the 186 river cross-sections in the Vu Gia Thu Bon River Basin.

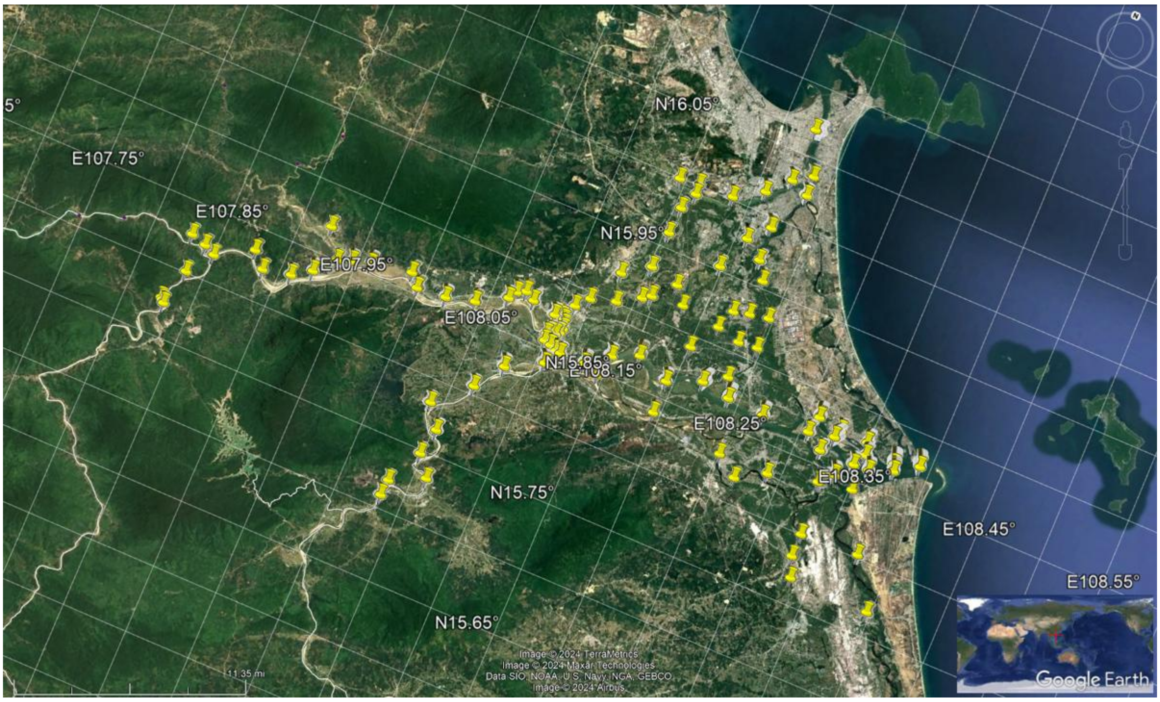

Figure A4. Locations of the flood trace data collection for the 2020 flood event.

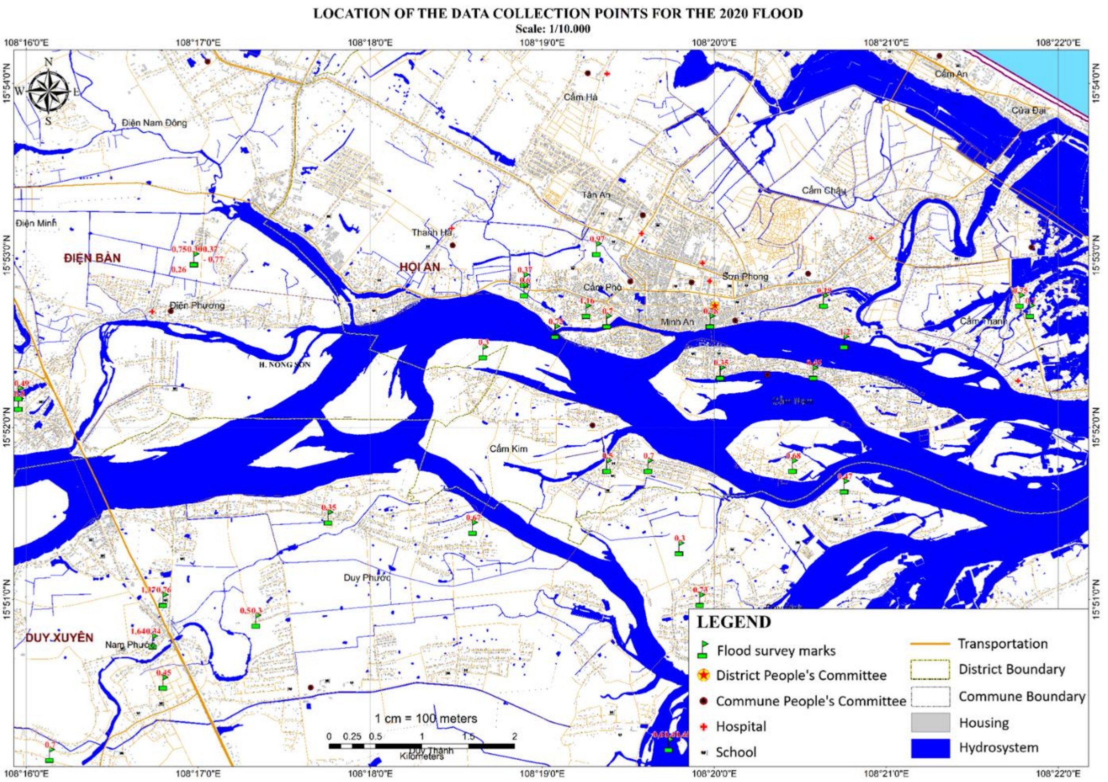

Figure A5. (a–f) Spatial distribution of floodwater depth across the floodplain for GWLs 2°C, 3°C, and 4°C (top to bottom), with the lower 25th (left) and upper 75th (right) percentiles of streamflow used as upstream boundary conditions.

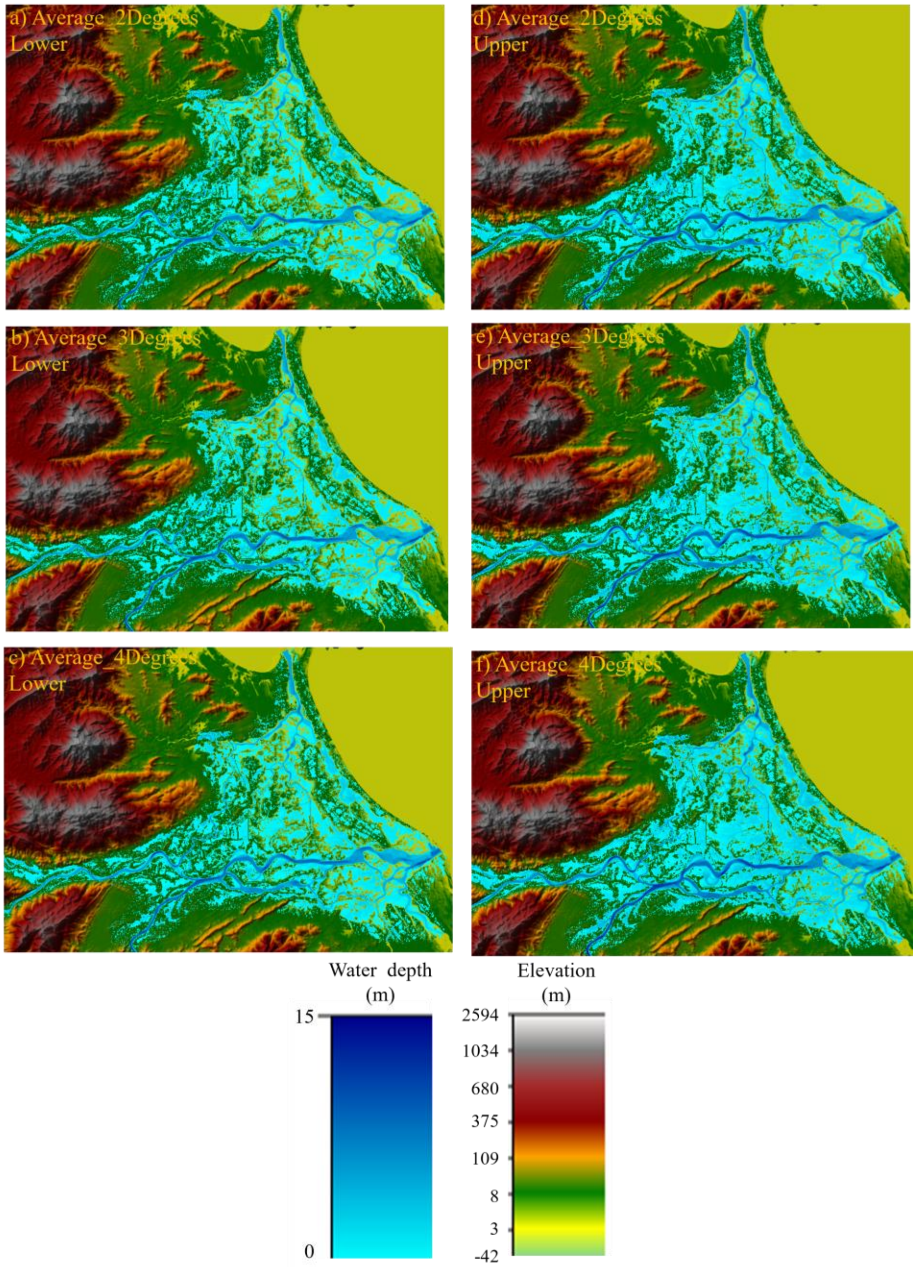

Agence française
de développement
5, rue Roland Barthes
75012 Paris l France
www.afd.fr

What is AFD?
Éditions Agence française de développement publishes analysis and research on sustainable development issues. Conducted with numerous partners in the Global North and South, these publications contribute to a better understanding of the challenges faced by our planet and to the implementation of concerted actions within the framework of the Sustainable Development Goals.
With a catalogue of more than 1,000 titles and an average of 80 new publications published every year, Éditions Agence française de développement promotes the dissemination of knowledge and expertise, both in AFD's own publications and through key partnerships. Discover all our publications in open access at editions.afd.fr.
Towards a world in common.

Publication Director Christophe Lecourtier
Editor-in-Chief Thomas Melonio

Legal deposit 3rd quarter 2026
ISSN 2492 - 2846

Rights and permissions
Creative Commons license
Attribution - No commercialization - No modification
https://creativecommons.org/licenses/by-nc-nd/4.0/

Graphic design MeMo, Juliegilles, D. Cazeils
Layout PUB
Printed by the AFD reprography service

To browse our publications:
https://www.afd.fr/en/ressources-accueil